UNIVERSITÀ POLITECNICA DELLE MARCHE

DIPARTIMENTO SCIENZE DELLA VITA E DELL'AMBIENTE

Corso di Laurea Magistrale in Biologia Marina

I mozziconi di sigaretta e il loro impatto sulla vitalità e biocalcificazione dei foraminiferi bentonici: risultati di test di tossicità acuta ed analisi di spettroscopia ad infrarossi

Cigarette butts and their impact on the vitality and biocalcification of benthic foraminifera: results of acute toxicity tests and infrared spectroscopy analyses

Tesi di Laurea Magistrale di:
Lucrezia Spaziani

Relatore
Prof.ssa Anna Sabbatini

Correlatore
Dott.ssa Francesca Caridi

Sessione straordinaria

Anno Accademico 2020/2021

TABLE OF CONTENTS

Da oltre 30 anni i mozziconi di sigaretta sono il rifiuto più comune al mondo: costituiscono fino al 90% dei rifiuti e spesso sono indicati come uno dei principali inquinanti di strade urbane e spiagge. Un singolo mozzicone può contaminare fino a 1000 litri d'acqua; il filtro, non essendo biodegradabile, si scompone e sminuzza, rimanendo nel mare per sempre con il suo carico di sostanze altamente tossiche tra cui la nicotina.

Per questo motivo, l'obiettivo di questa tesi è la valutazione degli effetti di una delle principali sostanze contenute nei mozziconi di sigaretta, la nicotina, sulla vitalità e sul processo di biomineralizzazione di organismi marini unicellulari eucariotici, i foraminiferi.

In particolare, sono state scelte tre specie di foraminiferi bentonici allevati in coltura e che in natura colonizzano gli ambienti marini costieri di tutto il mondo: *Rosalina globularis* e *Quinqueloculina* spp., che sono in grado di secernere un guscio di carbonato di calcio, e *Textularia agglutinans*, il cui guscio è costituito da particelle di sedimento che vengono selezionate dall'organismo stesso sulla base del substrato in cui vive.

Le specie selezionate di foraminiferi sono state fatte crescere in una soluzione di acqua di mare e nicotina sintetica per 48 ore.

L’analisi dell’impatto della nicotina sintetica sulle tre specie di foraminiferi ha previsto tre diverse fasi:

- Il tasso di mortalità delle tre specie è stato determinato attraverso due test di tossicità acuta (LC_{50}-48 h), a dicembre 2020 e ad aprile 2021, in cui i foraminiferi sono stati incubati in soluzioni stock di nicotina sintetica a concentrazioni subletali e letali (LC_{50}).
- Per rilevare la presenza di nicotina sintetica ed eventualmente del suo metabolita primario, la cotinina, nel mezzo di coltura dei precedenti test, è stato elaborato uno specifico protocollo per l’analisi con l’HPLC (High Performance Liquid Chromatography), messo in atto utilizzando i campioni del test LC_{50}-48 h di aprile 2021.
- Come ultimo step, per identificare i danni al guscio e alla cellula dei foraminiferi a carico della nicotina sintetica, alcuni campioni del test LC_{50}-48 h di aprile 2021 sono stati sottoposti a spettroscopia ad infrarossi (Fourier Transform Infrared, FTIR) presso il sincrotrone Elettra di Trieste.

Entrambi i test LC_{50}-48 h hanno dimostrato che la nicotina sintetica, sia a concentrazioni subletali che letali (LC_{50}), è tossica per tutte e tre le specie di foraminiferi. Per tutte e tre le specie è stato possibile definire un tasso di

mortalità, dal quale è emerso che *Quinqueloculina* spp. è la specie più resistente, mentre *R. globularis* e *T. agglutinans* sono le più sensibili.

Queste differenti risposte alla tossicità della nicotina sintetica sono specie-specifiche, in quanto legate al tipo di biomineralizzazione del guscio.

L'esame delle soluzioni del test LC_{50}-48 h di Aprile 2021 all'HPLC ha rivelato che i foraminiferi hanno assorbito fino al 90% della nicotina sintetica contenuta nei campioni; tuttavia, non sono state trovate alcune tracce di cotinina nel mezzo di coltura.

Le analisi al sincrotrone (FTIR), condotte su *T. agglutinans* e *R. globularis*, hanno invece evidenziato come la nicotina sintetica promuova l'indebolimento e la decalcificazione dei gusci e induca lo stress cellulare, alterando la composizione delle macromolecole citoplasmatiche (lipidi e proteine) nei foraminiferi sottoposti a questo inquinante considerato emergente.

Nel complesso, i risultati ottenuti in questa tesi magistrale hanno confermato il ruolo della nicotina come principale molecola intossicante contenuta nei mozziconi di sigaretta, in grado di intossicare i foraminiferi e di interferire con i loro meccanismi di biomineralizzazione.

Inoltre, il confronto di questi dati con studi ecotossicologici effettuati su altri organismi marini ha permesso di constatare che i foraminiferi bentonici sono sensibili alla nicotina e possono rappresentare un importante bioindicatore per l'inquinamento da mozziconi di sigaretta in mare.

1. INTRODUCTION

1.1 Foraminifera

Foraminifera constitute the most diverse group of shelled microorganisms in modern seas (Murray, 1991). They are protozoa (single-celled eukaryotic organisms), taxonomically designated as a phylum in the Kingdom of Protista. The estimated living species are about 10,000 (Vickerman, 1992). Of these, about 40 species are planktonic and the rest are benthic. They are ubiquitous in marine environments, from the intertidal to the deepest ocean trenches, and from the tropics to the poles.

Foraminifera's soft tissues (protoplasm) are enclosed within and protected by outer hard covering known as test (shell). Depending on the structure of the test, three basic wall compositions are recognised: organic (made by proteinaceous mucopolysaccharides), agglutinated (built using organically or calcitic cemented foreign material) and calcareous (secreted calcium carbonate in the form of calcite or aragonite). This latter incorporates important physiochemical properties of the life environment where foraminifera grew up. After their death, tests are preserved as fossils in the sediment.

The test can be organized in a single or several chambers (monothalamous or polythalamous). In polythalamous forms, each successive chambers are connected by an opening called foramen.

Another peculiarity of foraminifera is represented by granuloreticulose pseudopodia, ectoplasmic extensions with multiple functions, including locomotion, food capture, adhesion to substrate, formation of protective cysts and construction of the test (biomineralization).

Foraminifera have short reproductive cycle (six months to one year) (Boltovskoy,1964) and rapid growth (Walton, 1964). They can reproduce both asexually (through multiple fission: schizogony) and sexually (through gamogony and the subsequent fusion of biflagellate gametes).

1.2 Foraminifera as pollution bioindicators: general aspects

A bioindicator is an organism or biological response that reveals the presence of the pollutants by the occurrence of typical symptoms or measurable responses and is therefore more qualitative (Pati and Patra, 2012).

Benthic foraminifera are increasingly utilised as bioindicators, with particular interest for areas affected by strong anthropogenic impacts (Jorissen et al., 2018).

The advantage of application of foraminifera over other chemical and biological proxies for pollution monitoring can be summarized on the following points:

1. Their tremendous taxonomic diversity gives them the potential for diverse biological responses to various pollutants.
2. Due to relatively small size and great population diversity, statistically significant sample sizes can be collected quickly and relatively inexpensively for either faunal assemblage or for experimental studies, with minimal environmental impact.
3. Their short reproductive cycle and rapid growth make their community structure responsive to quick environmental changes.

4. Some species can be readily maintained in culture, so laboratory protocols can be established to determine responses of selected taxa to pollutants of concern.

5. They have biological defence mechanisms which protect them against unfavourable environmental factors, thus providing detectable biological evidence of the effects of pollution.

Further, foraminifera have an edge over the rest of the pollution monitoring techniques as the adverse effects of pollution could be incorporated into the calcareous tests; shells have an excellent preservation potential, thus providing concrete evidence for the presence and duration of existence of pollutants in an affected area and in the sedimentary records.

1.3 Applications of foraminifera in marine pollutants analyses

The employment of foraminifera as bioindicators of anthropogenic impact is constantly growing, as these microorganisms can perceive and respond to several forms of pollution in the marine environment.

These latter can be divided into three main categories:

- Organic pollution is due to the excessive input of nutrients and organic wastes through sewage systems into marine areas, leading to an exaggerated growth in primary production, resulting in eutrophication and oxygen depletion.
- Chemical pollution is linked to the toxic properties of artificially produced xenobiotics, like heavy metals, polycyclic aromatic hydrocarbons (PAHs), dioxins, polychlorinated biphenyls (PCBs) and pesticides. These compounds are usually non-biodegradable and highly persistent, so they are easily bioaccumulated by marine organisms.
- Anthropic pollution involves urban growth and associated activities, such as fishing, aquaculture, agriculture and industries. It includes thermal pollution as well, since power plants use a large amount of

water to cool the units, and heated water discharge returns to sea with a higher temperature (Issakhov and Zhandaulet, 2019).

Concerning foraminifera, their response to the previously described pollutants is investigated in two different ways:

- Through field studies (most frequent approach) focused on the ecological response of benthic foraminiferal fauna to these pollutants (i.e., variation of density, diversity and taxonomic composition).
- Through laboratory tests by setting up foraminiferal cultures and/or mesocosms, in which pollutants are directly given to these protists in the medium culture.

This second approach was applied in different studies to evaluate the effects of chemical pollutants, mainly heavy metals, on foraminifera.

Frontralini et al. (2018) performed a mesocosm experiment to assess the influence of lead on benthic foraminifera. Sediments bearing foraminiferal communities were incubated in mesocosms, exposed to different levels of lead in seawater, and monitored up to 8 weeks. Relatively high concentrations of lead seamed to affect foraminiferal communities by reducing their richness

or diversity, and the abundance of the most sensitive species as *Bolivina punctata* and *Porosononion granosum*.

A reduction in diversity was documented in a similar laboratory experiment with mercury (Frontalini et al., 2018) through both morphological and molecular (environmental DNA) analysis, and in a pilot mesocosm investigation, where foraminifera were exposed to different concentrations of copper (Frontalini and Coccioni, 2012). The experiment also revealed the biodiversity decreasing, and the increase of abnormalities in foraminiferal tests (e.g., reduced chamber size, aberrant chamber shape, abnormal additional chambers, or non-developed tests) considered a response of environmental and anthropogenic stress.

The symbiont bearing species *Amphistegina lessonii* was acutely (48 hours) exposed to dissolved zinc concentrations (de Freitas Prazeres et al., 2011). Despite no significant mortality was observed, a high percentage of individuals showed visual alterations (white spots or dark-brown areas in the tests) after the metal exposure. Three oxidative stress biomarkers (reactive-oxygen species generation, lipid peroxidation and total superoxide dismutase activity) were also analysed on this foraminiferal species.

As result, a lower competence against peroxyl radicals and oxidative damage was found in all experimental conditions except in the control group of

foraminifera (i.e., without zinc addition). Therefore, zinc induced the inhibition of *A. lessonii* defence mechanisms against oxidative stresses.

Nardelli et al. (2013) chronically (10 weeks) exposed the imperforated foraminifer *Pseudotriloculina rotunda* to zinc at six concentrations (between 0 and 100 mg/L), in order to understand the biological response of this species to the metal.

Increasing zinc concentrations led to increasing delay or to complete cease of the new chambers construction, with consequences on growth rates and affected vitality at medium to high concentrations. Despite this, zinc, even at high concentrations, did not cause test deformities due to anomalous arrangement of chambers.

An in vivo experiment, in which *Ammonia parkinsoniana* was incubated for up to 48 hours with different concentrations of cadmium, unravelled instead a progressive reduction in the pseudopodal activity and an increased accumulation of neutral lipids in the form of lipid droplets (Ros et al., 2020).

The same foraminiferal species was cultured in mesocosms and exposed over time (for 1, 3 and 8 weeks) to selected concentration of lead. *Ammonia parkinsoniana* specimens were evaluated at the cytological level. Through microscopy and dispersive spectrometer analyses, numerous morphological

differences, related to the pollutant-induced stress, were recognized between untreated (i.e., control) and treated (i.e., lead enrichment) samples. Higher concentrations of lead led to the increase of lipid droplets, proliferation of residual bodies, a thickening of the organic lining, mitochondrial degeneration, and the development of inorganic aggregates (Frontalini et al., 2015).

These examples evince foraminifera respond with cytological and shell alterations to the presence of high concentrations of heavy metals.

In the following paragraph I will introduce the problem of emerging pollutants and the state of the art in the use of foraminifera as bioindicators of the latter.

1.4 Emerging pollutants

Emerging pollutants (EPs), also known as contaminants of emerging concern (CECs), are a vast expanding array of anthropogenic compounds that are commonly present in water, but only recently has been identified as significant water pollutants (Gomes et al., 2018). No regulations are currently established for them (Tang et al., 2019).

As a result of the continuous development of anthropogenic activities, the production and use of emerging pollutants have increased.

The presence of emerging pollutants in the marine environment is the result of the uncontrolled urbanization, development of industry, health care activities essential to support human well-being, agriculture and transport, and include a wide range of substances produced by humans, considered indispensable for the modern society (Vasilachi et al., 2021).

EPs are synthetic persistent organic chemicals, including pharmaceuticals, personal care products, pesticides, household products, surfactants, microplastics and nanoparticles, industrial additives and solvents (Luo et al., 2014; Vasilachi et al., 2021).

Many of them are continuously released into the marine environment without being monitored, and even in very low quantities they may create adverse effects on the aquatic wildlife and human health.

The emerging pollutants represent novel substances as well as the main source of anthropogenic litter.

Marine debris, as anthropogenic litter, is also a global environmental issue. Chemistry of water and sediments, thus environmental quality and eventually the trophic chain, are affected by dispersal of plastics and chemicals (Cau et al., 2020). For example, smoked cigarette butts (CBs) are the predominant human coastal litter item together with plastic debris and associated substances that can be bioaccumulated in marine organisms (Li et al., 2018; Araújo and Costa, 2019).

1.4.1 Cigarette butts

Cigarette butts (CBs) are the most common form of personal litter in the world, as trillion cigarettes are smoked every year worldwide (Curtis et al., 2017). 4,5 trillion cigarettes are annually littered in the environment, and it is expected that these wastes would increase by 50% until 2025.

Cigarette waste constitutes an estimated 30% of the total litter on US shorelines, waterways, and on land (Litter Free Planet, 2009). Research

carried out between 2002 and 2006, as part of United Nations Environment Program (UNEP), showed that cigarette butts rank first in the top ten of the most abundant litters in the Mediterranean (Lombardi et al., 2009).

The existence of CB wastes in different areas increases the environmental risks and the transmission of contaminants into the environment (Moerman and Potts, 2011).

Their impact is related to their small size, persistence in the environment (mostly due to cellulose, plastic fibres and other no-biodegradable materials constituting cigarette filters), potential toxic effects (Lee, 2012), and their chemical composition.

There are over 5000 compounds present in cigarettes. Among these, at least 150 are considered to be highly toxic, mainly because of their carcinogenic and mutagenic properties (Slaughter et al., 2011).

When burned, many of the chemicals present in cigarettes produce new compounds (Novonty et al., 2009). The compounds with the highest toxic potential are mainly concentrated in the remains of the tobacco and in the filter (Slaughter et al., 2011). They can contaminate the soil after leaching by rainwater and are superficially transported to aquatic environments where they can be detected.

Some of the chemicals found in the cigarette particulate matter (tar) and in the mainstream smoke are hydrogen cyanide, nitrates, ammonia, acetaldehyde, formaldehyde, benzene, phenol, pyridine, carbon monoxide, polycyclic aromatic hydrocarbons (PAHs), carbon monoxide, amines, heavy metals (Lee and Lee, 2015).

The origin of contaminants in CBs comes from the different stages of tobacco cultivation, processing and manufacturing of cigarettes. These substances are indeed added naturally to cigarettes during the different processes (Dieng et al., 2013). Some toxins (such as nicotine) naturally exist in the tobacco leaves, while others (for instance heavy metals) are adsorbed by tobacco from soil and fertilizers during plant growth.

Further, some xenobiotics present in cigarettes result from the materials previously added to the plant including fungicides, herbicides, insecticides, and pesticides (Dieng et al., 2014).

Approximately two-thirds of cigarette butts are released directly into the environment by smokers and not destroyed into solid waste management systems (Novotny and Slaughter, 2014). Hence, these deposited debris may eventually reach freshwater and marine basins.

Distribution and diffusion of CBs and their associated compounds in the aquatic environment could be a threat to various animal and plant species. For instance, CBs have been found in the stomach contents of marine fauna that accidentally ingested them during feeding (Santos et al., 2005).

Besides physical injuries, the toxic tobacco chemicals could be also desorbed out from deposited CBs and pose additional threats to wildlife health (Figure 1).

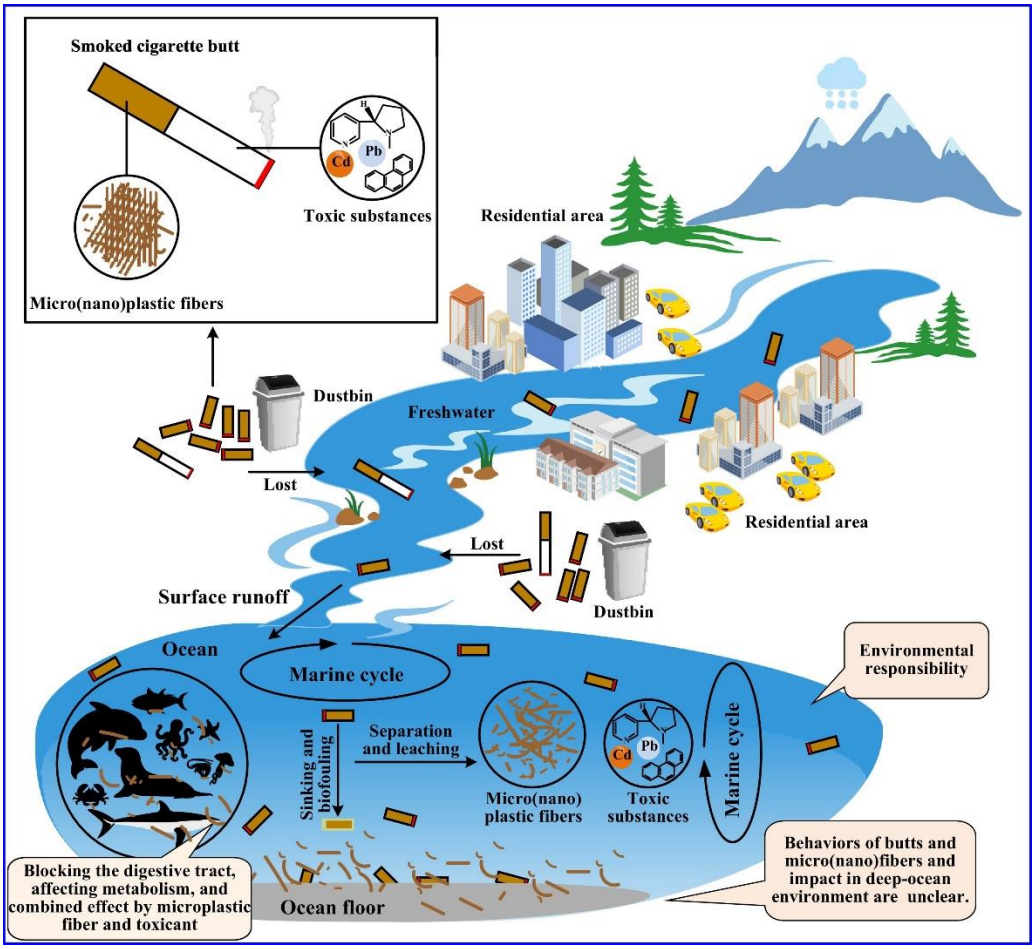

Figure 1. Fates and potential effects of smoked cigarette butts in the environment (Shen et al., 2021)

1.5 Foraminifera as indicators of emerging pollutants

The literature shows that despite the growing interest in marine litter, this specific issue remains little studied, and information is limited in time and space. Studies have been undertaken on islands, continental coasts, estuaries, and coastal cities (see Araújo and Costa, 2019 and Table I therein) with a wide variety of approaches to classification against zero attempts of modelling their dispersion in marine environment; for instance, CBs are considered plastic in 19% of studies and placed in an isolated category in another 16%. Moreover, it is possible to identify the main sources of CBs in coastal and marine environments, but little is known on the toxicity on marine biota, and in particular to biocalcifying taxa as foraminifera, target of this master's degree thesis.

Very few experimental studies have so far documented the effects of emerging pollutants on foraminifera, and none of them concerns cigarette butts and nicotine contained in them.

The average cigarette contains 0.8–1.9 mg of nicotine. This delivers a human dose when smoked of 10–30 μg kg^{-1} based on an average adult weigh of 68 kg, resulting in average peak plasma levels of 10–50 ng ml^{-1} (Wright et al., 2015). Preliminary results proved that there is an acute toxicity (LC_{50}-48 h) of human-smoked CB leachate on three cultured genera of benthic foraminifera:

the calcareous perforate *Rosalina globularis*, the calcareous imperforate *Quinqueloculina* spp., and the agglutinated *Textularia agglutinans*. The specimens were exposed to 16, 8, 4, 2, and 1 CBs/L concentrations (corresponding to 31.25, 15.63, 7.82, 3.91, 1.96 mg of nicotine/L).

Starting from 4 CBs/L, both calcareous genera showed shell decalcification, and death of almost all the individuals, except for the more resistant agglutinated species.

By means of FTIR (Fourier Transform Infrared) spectroscopy analysis we demonstrated that foraminiferal death and decalcification could be an interplay of the pH reduction due to the CB leachate and the toxicity of other dissolved substances, in particular nicotine, which lead to physiology alteration and in many cases cellular death (Caridi et al., 2020).

In this master's degree thesis, I intend to deepen these first important results with acute toxicity assays (LC_{50}-48 h) performed using synthetic nicotine leachate in order to assess the potential effect of this single parameter.

Nicotine is neurotoxic, affecting the central and autonomic nervous system and neuromuscular junctions by agonistically (Matta et al., 2007) binding to the nicotinic acetyl cholinergic receptors (nAChRs). This opens ion channels,

causing an influx of sodium or calcium ions, increasing the release of neurotransmitters.

Foraminifera, as unicellular animals, may not have these receptors, but they have ion channels (i.e., calcium) in their cellular membrane supporting the biomineralization process. Keul and Schimdt (2018) demonstrated that two calcareous perforate foraminiferal species were highly sensitive to a calcium channel blocker, clearly indicating that the majority of calcium ions needed during calcification is taken up via trans-membrane transport.

Moreover, this experiment will let me to assess if the nicotine could be considered a biomarker of exposure to the toxicants associated with smoking.

I aim to evaluate the presence of nicotine in the medium culture as indirect measure of foraminiferal nicotine metabolism together with its potential inhibition to biocalcification.

2. OBJECTIVES

As previously mentioned, except for Caridi et al.'s work (2020), studies on foraminifera phylum investigating the toxicity of cigarettes butts have not been performed yet.

Starting from this study, the aim of this master's degree thesis is to evaluate the effects of synthetic nicotine on three selected species of benthic foraminifera (*Rosalina globularis*, *Quinqueloculina* spp., *Textularia agglutinans*) with a particular focus on their vitality and possible changes in their biocalcification rates.

In order to do this, two acute toxicity tests (LC_{50}-48 h) were conducted by replacing CB leachate as used in Caridi et al. (2020) with a synthetic nicotine stock solution. In particular, we considered only sublethal and lethal (LC_{50}) concentrations of synthetic nicotine, derived from the previous experiment.

To evaluate the effects of this emerging pollutant on the biocalcification rates, infrared spectroscopy (FTIR) analyses were conducted.

In addition, using High Performance Liquid Chromatography (HPLC), a protocol was developed for assessing the presence of synthetic nicotine and possibly its main catabolite, cotinine, in the solutions in which the foraminifera were grown.

3. MATERIALS AND METHODS

3.1 Experimental design

The potential toxicity of chemical substances is often presented as their LC_{50}, which is the concentration of a substance that is lethal to 50% of the organisms. LC_{50} test is one of the most effective analyses to assess the acute toxicity effects of emerging pollutants on marine organisms, as demonstrated by numerous studies conducted on many marine taxa with different contaminants. In a toxicity test the percentages of mortality obtained revealed a degree of toxicity ranging from highly toxic to non-toxic in the organisms (Boyd, 2005).

The experiments were conducted in December 2020 and April 2021, taking the work of Caridi et al. (2020) as reference.

In the latter, the gas chromatography-mass spectrometry (GC-MS) analysis of a cigarette butt stock solution (used in the preparation of the experimental treatments) revealed that the leachate contained predominantly nicotine at a high concentration (62.5 mg/L).

Consequently, in the experiment described in this thesis, only synthetic nicotine was considered, in order to determine whether this substance can be the main responsible for both cellular stress and decalcification effect.

To test this hypothesis, specific protocols were developed:

1) In the experiment of December 2020 only LC_{50}-48 h test was performed to detect synthetic nicotine concentrations and mortality effects. This first protocol intends to deepen the first important results achieved by Caridi et al. (2020) with acute toxicity assay (LC_{50}-48 h) performed using synthetic nicotine to assess the potential effect of this single parameter.
2) In the April 2021 experiment, in addition to the acute toxicity test (LC_{50}-48 h), the protocols for HPLC and synchrotron analysis on selected foraminiferal individuals were implemented and enacted.

   This second protocol was tested to assess if the nicotine could be considered a biomarker of exposure to the toxicants associated with smoking. In particular, it evaluates the presence of nicotine metabolite, cotinine, in the medium culture as indirect measure of foraminiferal nicotine metabolism together with its potential inhibition to biocalcification using HPLC and synchrotron.

3.1.1 Foraminiferal cultures

Three different species of foraminifera, characterized by different typologies of shell calcification, were selected for this study.

Rosalina globularis is a perforate calcareous species which precipitates $CaCO_3$ to build its test; its shell is usually made of low Mg calcite and this group is perforate with numerous microscopic pores that are found in most of the surface area of the shells (Erez, 2003).

Rosalina globularis is a monolamellar species. Its calcification mechanism starts from the formation of the primary organic membrane (POM), a thin layer of organic matrix partially isolating the organism from its environment. POM acts as template for the nucleation and precipitation of $CaCO_3$ (Sabbatini et al., 2014).

Quinqueloculina spp. is an imperforate (miliolid/porcellanaceous) foraminifer; miliolids precipitate their needle-shaped calcite crystals (usually high Mg calcite) within intracellular vacuoles.

Textularia agglutinans is an agglutinated foraminifer that allocates particles of different type and size in a sufficient quantity to create a new case gluing them with a biomineralized calcium carbonate cement (Sen Gupta, 1999).

Foraminiferal cultures were maintained in glass beakers with seawater filtered with a 0.42 mm membrane filter at pH of about 8.0, adjusted in salinity of 37 at room temperature to obtain reproduction and subsequent growth of the juvenile population. To reduce the fast increase of salinity and the accumulation of organic waste products, the culturing beakers were refilled by replacing about 20-40% of original seawater. Measures of salinity and temperature were performed weekly, and salinity was corrected by adding deionized water when necessary.

All cultures were fed every fortnight with a few drops of freezed-killed concentrated algae (*Isochrysis galbana*).

3.1.2 Preparation of the stock solution

The stock solution for the acute toxicity test (LC_{50}-48 h) was prepared by adding 10 mL of a 35% mass/volume synthetic nicotine solution (Nicotine hemisulfate salt, Sigma Aldrich) to 90 mL of artificial seawater to obtain a synthetic nicotine concentration of 35 g/L (1:10 dilution).

The artificial seawater was made adding 2 L of deionized water and 75 g of Instant Ocean® and after an overnight stabilization, yield a pH range between 8.0 and 8.4 and a salinity range of 35-37 ppt.

3.1.3 Foraminiferal LC_{50} tests

In Caridi et al.'s work (2020), chemical analyses were conducted to determine the presence and the concentration of nicotine in the utilized CB leachates.

By using a gas chromatography-mass spectrometry (GC-MS) analysis, a nicotine concentration of 62.5 mg/L was determined in the stock cigarette butt infusion.

From the initial sublethal and lethal concentrations obtained by Caridi et al. (2020), the corresponding amounts of synthetic nicotine (mg/L) were derived for each species.

1 CB/L: 1.96 mg nicotine/L = *R. globularis* sublethal concentration: X

1 CB/L: 1.96 mg nicotine/L = 1 CB/L: X → 1.96 mg/L

1 CB/L: 1.96 mg nicotine/L = *Quinqueloculina* spp. and *T. agglutinans* sublethal concentration: X

1 CB/L: 1.96 mg nicotine/L = 2 CBs/L: X → 3.91 mg/L

1 CB/L: 1.96 mg nicotine/L = *R. globularis* LC_{50}: X

1 CB/L: 1.96 mg nicotine/L = 1.9 CBs/L: X → 3.72 mg/L

1 CB/L: 1.96 mg nicotine/L = *Quinqueloculina* spp. LC_{50}: X

1 CB/L: 1.96 mg nicotine/L = 7.2 CBs/L: X → 14.11 mg/L

1 CB/L: 1.96 mg nicotine/L = *T. agglutinans* LC_{50}: X

1 CB/L: 1.96 mg nicotine/L = 5.6 CBs/L: X → 10.98 mg/L

For each concentration, the volume of stock solution was then calculated for a final volume of 40 mL (the volume of jars in which foraminifera were placed during the toxicity test) (Table 1). In particular, the dilution formula was applied ("C" stands for concentration, "V" stands for volume) to obtain the initial volumes of stock solution.

$$C_1V_1 = C_2V_2 \rightarrow V_1 = C_2V_2/C_1$$

	Rosalina globularis	***Quinqueloculina* spp.**	***Textularia agglutinans***
CONTROL	0 µL	0 µL	0 µL
SUBLETHAL	2.24 µL	4.46 µL	4.46 µL
LC_{50}	4.2 µL	16 µL	12.5 µL

Table 1. Volumes of stock solution for a final volume of 40 mL.

The foraminiferal specimens belonging to the three species were picked from cultures with a fine brush and insert in small plastic jars (with a volume of 40 mL) previously prepared with the artificial seawater.

In the experiment performed in December 2020, for all three genera considered, 3 replicates for both lethal and sublethal concentrations of synthetic nicotine were taken, plus one control concentration (without

nicotine stock solution inside). Each replicate contained 5 individuals, giving a total of 35 individuals of foraminifera for each species (Figure 2).

The same experiment was conducted in April 2021, but all *T. agglutinans* replicates contained only 3 individuals, due to the low number of individuals of this species found during the picking phase (probably the reproductive rate of *T. agglutinans* at that time was not particularly high).

In both experiments, after picking, all foraminifera were observed under both the stereomicroscope and the light microscope to verify that they were alive (based on the coloration of foraminifera and pseudopodial activity) (Figure 3 and Figure 4).

Before starting the test, volumes of artificial seawater equal to the previously calculated volumes of synthetic nicotine stock solution (Table 1) were removed from each jar, then the corresponding volumes of stock solution were added to the samples (excluding the control).

The test (LC_{50}-48 h) was run under laboratory controls: water quality readings (temperature, salinity, and pH) of all jars were performed before and after the experiment.

After the experimental treatments, survival count was performed following the Ross and Hallock method (2018). All foraminiferal specimens were

removed from jars by brush, and they were rinsed with clean seawater three times to remove residuals of nicotine stock solution.

Then, they were put in Petri dishes with 15 mL filtered seawater and 0.4 μL of fluorescent probe Cell Tracker Green (CTG) for 30 minutes.

Cell Tracker Green is a vital fluorogenic probe that was developed to exclusively stain living cells (Bernhard et al., 2006).

When living cells are incubated in CTG, the probe passes through the cellular membrane and reaches the cytoplasm, where nonspecific esterase hydrolyses the probe to produce the fluorescent compound, that can be microscopically viewed after excitation at the appropriate wavelengths (Pucci et al., 2009).

The requirement of esterase activity means that a cell must be alive to produce fluorescence (Ross and Hallock, 2018).

Soon after, the foraminifera were again rinsed with clean seawater to remove any remaining CTG and checked for cellular activity using a fluorescence binocular microscope.

The foraminiferal specimens were then maintained for 72 hours in clean seawater, following the protocols developed by Ross and Hallock (2012), and colour and activity of each individual were visually assessed to identify possible quiescent organisms (recovery phase).

Quiescence is a subset of dormancy (Ross, 2012) induced by exogenous factors (i.e., a reaction to environmental stressors).

This life strategy involves suspension of metabolic processes, arrested development, pseudopodia withdrawing and lack of movement (Ross, 2012; Ross and Hallock, 2016).

Quiescence differs from death, because it allows foraminifera to restore their vital activities following the return of favourable environmental conditions.

The recovery phase is essential to distinguish dead individuals from survivors, so that LC_{50}-dead individuals can be excluded from the count.

In fact, the next step was to count the live and dead foraminifera for each concentration in order to construct vitality graphs, which display the percentage of live individuals in the samples.

In the April 2021 experiment, some samples were not stained with Cell Tracker Green, to avoid possible interference with the subsequent synchrotron analysis: all the third replicates (R3) and one individual of each control.

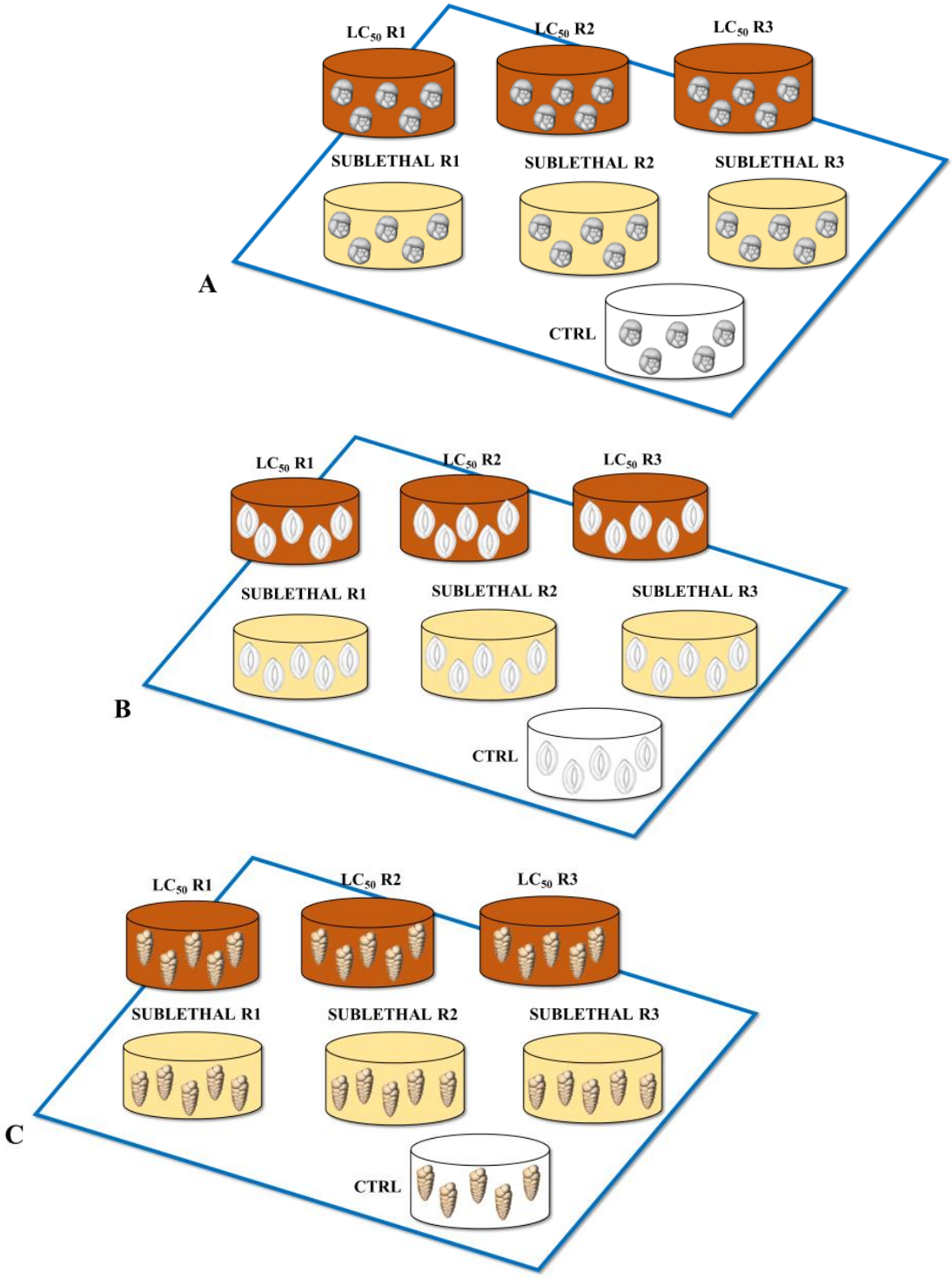

Figure 2. Schematic design of the LC_{50}-48 h test performed in December 2020. The plates represent the three different species: A) *Rosalina globularis*; B) *Quinqueloculina spp.*; C) *Textularia agglutinans*. Each jar coincides with a specific sample and each colour indicates the synthetic nicotine concentration inside the samples: white is for control (without synthetic nicotine), yellow is for the sublethal concentration, brown is for the LC_{50}. The exact amounts of synthetic nicotine used in the test are reported in Table 1.

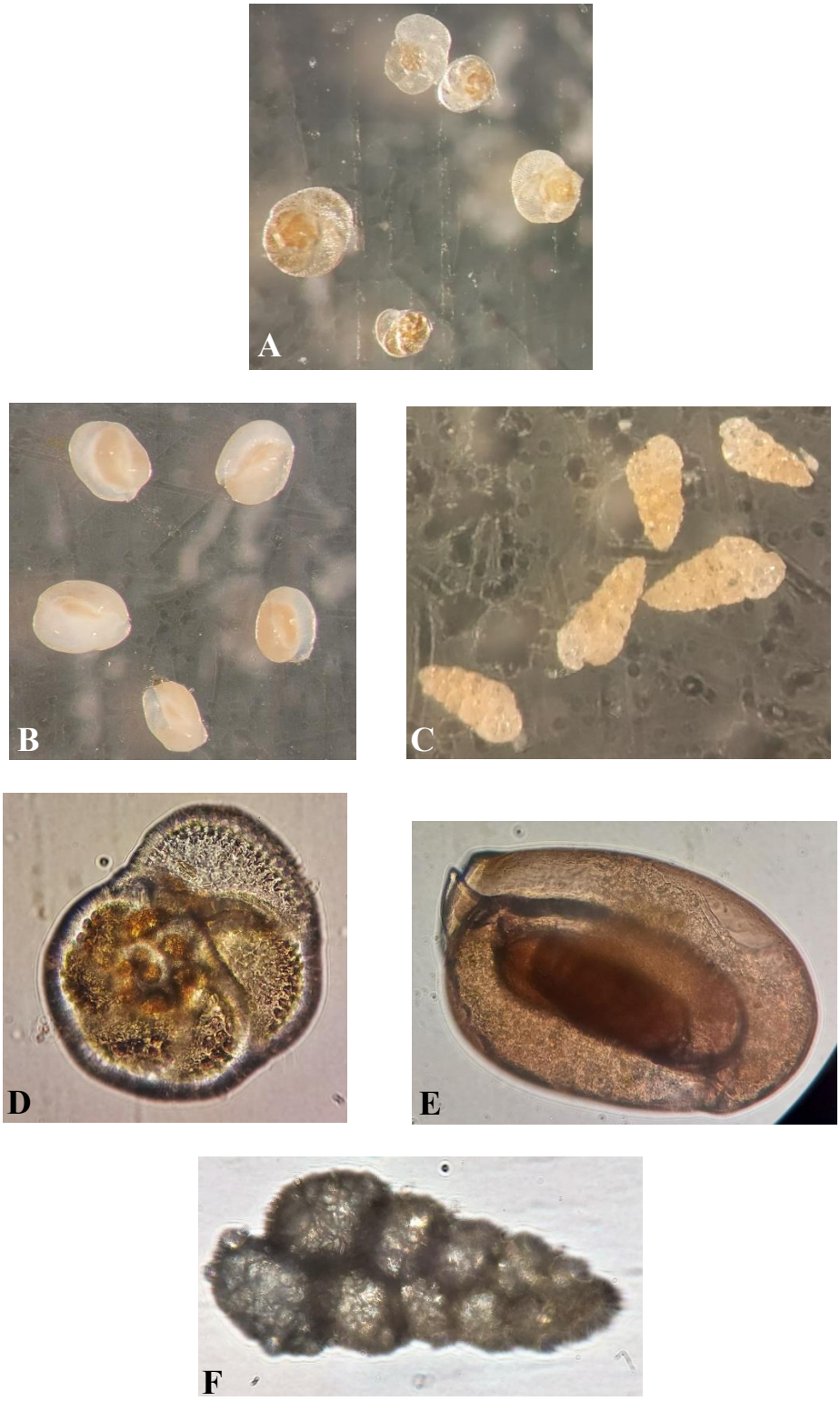

Figure 3. Foraminiferal species before the LC_{50}-48 h test (December 2020) observed under the stereomicroscope (A, B, C) and optical microscope (D, E, F) respectively. The species are: *Rosalina globularis* (A, D); *Quinqueloculina spp*. (B, E); *Textularia agglutinans* (C, F).

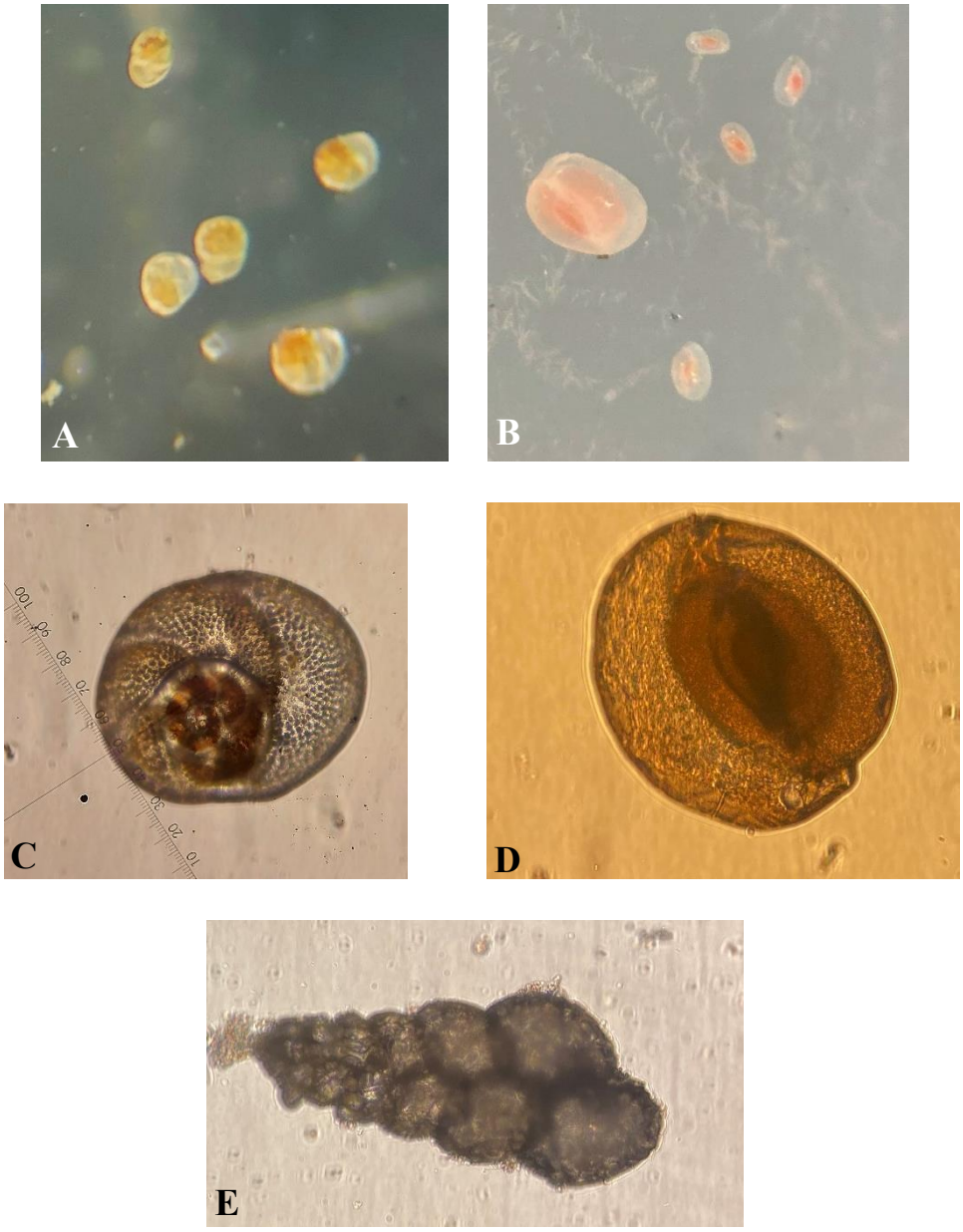

Figure 4. Foraminiferal species before the LC_{50}-48 h test (April 2021) observed under the stereomicroscope (A, B) and optical microscope (C, D, E) respectively. The species are: *Rosalina globularis* (A, C); *Quinqueloculina spp*. (B, D); *Textularia agglutinans* (E).

3.2 Chemical analyses on stock solutions

3.2.1 HPLC

The HPLC at the Department of Specialist Clinical and Odontostomatological Sciences (DISCO) of Polytechnic University of Marche (Figure 5) was operated at 45.9°C to detect the presence of nicotine and its main metabolite, cotinine, in the culture medium in which the foraminifera were incubated during the acute toxicity test.

HPLC is an instrument able to separate, identify and quantify compounds that are dissolved in a mixture.

The solvent used to separate components in a liquid sample for HPLC analysis is called mobile phase. The latter is delivered to a separation column with packing material, otherwise known as stationary phase, and then to the detector at a stable rate controlled by the solvent delivery pump. A certain amount of sample is injected into the column and the compounds contained in the sample are separated.

The compounds separated in the column reach a detector downstream of the column and each compound is identified and quantified.

Sample retention time (the time it takes for the molecules to reach the detector) may vary depending on the interaction between the stationary phase,

the molecules being analysed, and the solvent used. As the sample passes through the columns, it interacts between the two phases at different rate, primarily due to different polarities in the analytes.

In the column, the stronger the affinity between a component of the mixture and the mobile phase, the faster the component moves through the column along with the mobile phase (lower retention time). On the other hand, the stronger the affinity with the stationary phase, the slower it moves through the column (higher retention time).

The specific HPLC used in the analysis described below consists of the following parts:

- Autosampler HT300L (HTA)
- Binary pump YL9110 (Young Lin)
- Diode array detector SPD-M10Avp (SHIMADZU)
- Detector controller SCL-10Avp (SHIMADZU)
- Column Synergi^{TM} Fusion RP-80, 250 x 4.6 mm (Phenomenex)
- Integration software YL-Clarity (Young Lin)

Figure 5. HPLC at the Department of Specialist Clinical and Odontostomatological Sciences (DISCO) of Polytechnic University of Marche.

The first step in the protocol developed for this thesis was the preparation of mobile phases A and B. In a beaker containing 1 L of MilliQ water, 6.80 g of 50 mM KH_2PO_4 and 1.01 g of 5 mM heptane sulfonate were added. The pH of this solution was raised to 6.1 using 4 KOH tablets, one of which was diluted in 1 mL of MilliQ water.

The solution was transferred to a graduated cylinder and its volume was increased to 1 L; it was then filtered and degassed using a vacuum filtration pump. Part of this solution (540 mL) was used as mobile phase A, which was placed in a plastic container connected to the HPLC. The remaining 460 mL was used to obtain mobile phase B. Specifically, the 460 mL represented 60% of the final volume, to which 40% methanol was to be added.

Applying the proportion 60: 100 = X: 460 mL, a final volume of 766.66 mL was calculated. Consequently, 306.66 mL of methanol was added to the remaining 460 mL to achieve a 40% methanol concentration.

Before loading phase B into the HPLC, the graduated cylinder was sealed with parafilm, then the solution was shaken and degassed with the vacuum pump.

As a second step, three standard solutions were prepared, containing nicotine salt, pure nicotine and cotinine respectively.

The standards were prepared in 1 mL eppendorf tubes. The volume to be included in a final concentration of 20 mM was determined for each compound.

- Nicotine salt (nicotine hemisulfate salt, 35% w/v in H_2O) has a molecular weight of 422.54 g/mol. To convert the molecular weight to mass, the following formula was applied:

$$\frac{422.54 \frac{\text{g}}{\text{mol}} * 20 \text{ mM}}{1 * 10^6} = 0.0084 \text{ g} \rightarrow 8.4 \text{ mg}$$

For an initial 35% w/v concentration of nicotine in salt, the volume of nicotine in the standard solution was derived as follows:

$$\frac{8.4\ \text{mg}}{35 * 100} = 24\ \text{mg}\ \rightarrow 24\ \mu\text{L}$$

Accordingly, 986 µL of mobile phase A and 24 µL of nicotine salt were placed in the eppendorf.

- Pure nicotine has a molecular weight of 162.24 g/mol. Its molecular weight has been converted to mass:

$$\frac{162.24\frac{\text{g}}{\text{mol}} * 20\ \text{mM}}{1 * 10^6} = 0.0032\ \text{g}\ \rightarrow 3.2\ \text{mg} = 3.2\ \mu\text{L}$$

For convenience, a weight of 5 mg was considered; then, applying the dilution formula ($V_1C_1 = V_2C_2$), the final volume of pure nicotine to be included in the standard solution was derived:

$$1\text{: } 3.2\ \text{mg} = \text{X: } 5\ \text{mg} \rightarrow \text{X} = 1.56\ \mu\text{L}$$

- Cotinine has a molecular weight of 176.22 g/mol. The molecular weight has been converted to mass:

$$\frac{176.22\frac{\text{g}}{\text{mol}} * 20\ \text{mM}}{1 * 10^6} = 0.0034\ \text{g}\ \rightarrow 3.4\ \text{mg} = 3.4\ \mu\text{L}$$

Again, a mass of 5 mg was taken into account; then, by reapplying the dilution formula ($V_1C_1 = V_2C_2$), the final volume of cotinine to be included in the standard solution was obtained:

$$1: 3.4 \text{ mg} = X: 5 \text{ mg} \rightarrow 1.47 \text{ µL}$$

These standards were loaded onto the HPLC to obtain graphs describing the absorbance over time of each of the three compounds, in order to compare the peaks obtained with those of each acute toxicity test (LC_{50}-48 h) sample.

Before loading all samples, the HPLC parameters for the analysis were set as follows:

- Gradient curve
- 40% methanol
- T = 45.9°C

The samples were loaded onto the HPLC, each with a volume of 200 µL, by first placing the control (with only MilliQ water) and then the three standards (in order: nicotine salt, pure nicotine, cotinine). As previously set up, the instrument analysed an aliquot of 30 µL for each sample and the VWD detector was set at 260 nm, the wavelength at which nicotine and cotinine reach the maximum absorbance.

After identifying the absorbance peaks over time for each of these first samples, three solutions, defined as Mix, were made to understand if the instrument was able to detect the standard peaks, within a mix solution, maintaining the same characteristics (absorbance and retention time):

- Mix 1 = nicotine salt (5 µL) + cotinine (5 µL) + mobile phase B with 18% methanol (990 µL)
- Mix 2 = nicotine salt (5 µL) + cotinine (5 µL) + mobile phase B with 18% methanol (990 µL)
- Mix 3 = nicotine salt (5 µL) + cotinine (5 µL) + pure nicotine (5 µL) + mobile phase B with 18% methanol (958 µL).

To each mix a concentration of 3 mol KCl was added to bring forward the peaks, the volume of which was obtained by applying the dilution formula ($V_1C_1 = V_2C_2$):

$$3 \text{ mol: } X = 0.1\text{: } 1 \text{ mL } (+X) \rightarrow X = 30 \text{ µL}$$

This resulting volume was added to 970 µL of each of the three mixes.

The Mix 3 + KCl was used as a control for our analyses.

In order after the control, the experimental samples of the LC_{50}-48 h test were loaded onto the HPLC, which were previously processed through the following steps:

- Samples were lyophilized, by using the freeze-dryer model LIO-5P 4K (5Pascal) available at the Department of Specialist Clinical and Odontostomatological Sciences (DISCO) of Marche Polytechnic University.

Lyophilization consists in dehydrating a substance through cryodesiccation. It is a process in which water is removed from a product after it is frozen and placed under a vacuum, allowing the ice to change directly from solid to vapor without passing through a liquid phase (Beaty, N., 2006).

- 4 mL of mobile phase (2 mL of phase A and 2 mL of phase B) with 20% methanol were added to each one
- Mixing for 10 minutes
- Sonication for 1 minute, keeping samples on dry ice
- The content of each sample was transferred to four 1 mL eppendorfs to be centrifuged for 10 minutes (at 22000 rpm). Subsequently, the supernatant was transferred to three more eppendorfs and 200 µL was utilized for HPLC analysis.

At the end, form all chromatograms, describing the absorbance (mAu) over time (min), the areas under the curves were estimated and were used to calculate the synthetic nicotine recovery rate (N%). This area is normally proportional to the quantity or concentration of the eluted substance.

To determine the synthetic nicotine recovery rate for each sample, the initial (μmol_i) and total (μmol_t) nicotine concentrations were calculated as follows:

$$\mu mol_i = \frac{\mu L * d * \frac{35}{100}}{PM} * 1000$$

where μL is the initial synthetic nicotine concentration used for the experiment; d is the nicotine salt concentration; $35/100$ is the nicotine salt concentration.

$$\mu mol_t = \frac{Nc\ (nmol)}{30\ \mu L * 4000/1000}$$

where Nc is the synthetic nicotine concentration; $30\ \mu L$ is the aliquot analysed by the instrument; $4\ mL$ is the volume of mobile phase added to each sample.

The synthetic nicotine concentration expressed in nmol is calculated used the standards values (areas and concentration) as:

$$nmol_s : area_s = X : area_e$$

where $nmol_s$ is the initial concentration of nicotine used to set up the standards; $area_s$ is the chromatogram area of the nicotine standard; $area_e$ is the chromatogram area of the sample.

$$N\% = \frac{\mu molt}{\mu moli} * 100$$

3.2.2 Fourier Transform Infrared analyses

In the experiment performed in April 2021, to assess cell damage and quantify the possible loss in calcium carbonate that the three foraminiferal genera underwent, Fourier Transform Infrared (FTIR) analysis was used. Foraminifera samples were measured at SISSI beamline, biochemical and life sciences branch (SISSI-bio) at Elettra Sincrotrone Trieste (Figure 6).

(Samples employed in this analysis are reported in the FTIR supplementary data).

Samples were inspected under an optical microscope, Zeiss Stemi 305, and then transferred onto the Diamond compression cell (ST Japan). There, the two halves of the cell were placed on the top of the other and the samples slowly compressed between the two diamonds. When the sample is pulverized and compressed enough to be measured to be measured in transmission mode, the cell was opened and put under the Hyperion 3000 optical/infrared microscope (Bruker Optics) to be measured. For each sample, the whole imprint left on the face of the compression cell was measured in imaging mode with a 64 x 64-pixel Focal Plane Array (FPA), collecting 128 scans at 4 cm^{-1} spectral resolution. The pixel size acquired with 15x IR/VIS objective/condenser Cassegrain optics is 2.66 x 2.66 μm. For smaller samples,

imaging before closing the cell was performed with the same acquisition parameters described before.

The sequence in Figure 7 shows the sample preparation. An individual is removed from the vial using a pipette and dropped onto one-half of the opened diamond cell (7A) and using the tweezers or a needle put in the center of the diamond window (7B). Then when the water is evaporated, the sample is broken with a needle, avoiding losing material (7C-D) and then the second half of the cell put on top of the first and the sample pulverized slowly (7D), finally the three screws of the cell are tightened and the sample flattened (7F). After this, the compression cell is opened and the material adhering onto the two faces of the diamonds measured in transmission mode. This procedure will allow for a more homogeneous layer thickness and to avoid saturation of the strong absorbing bands of calcium carbonate.

After all the data were acquired, they were corrected in OPUS software (Bruker Optics) for water vapor and CO_2 contributions to the spectra.

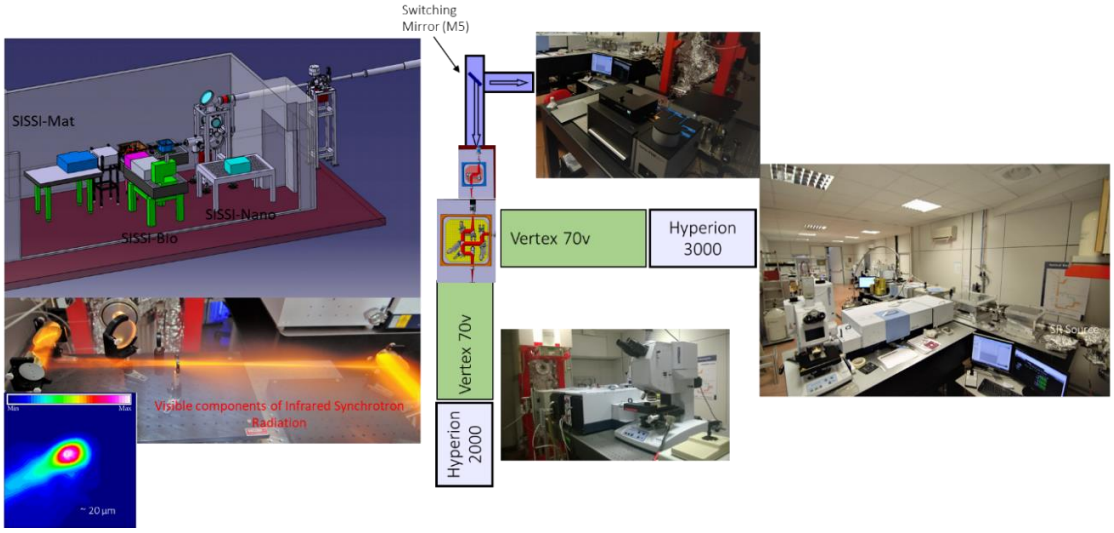

Figure 6. SISSI beamline at Elettra Sincrotrone (Trieste)

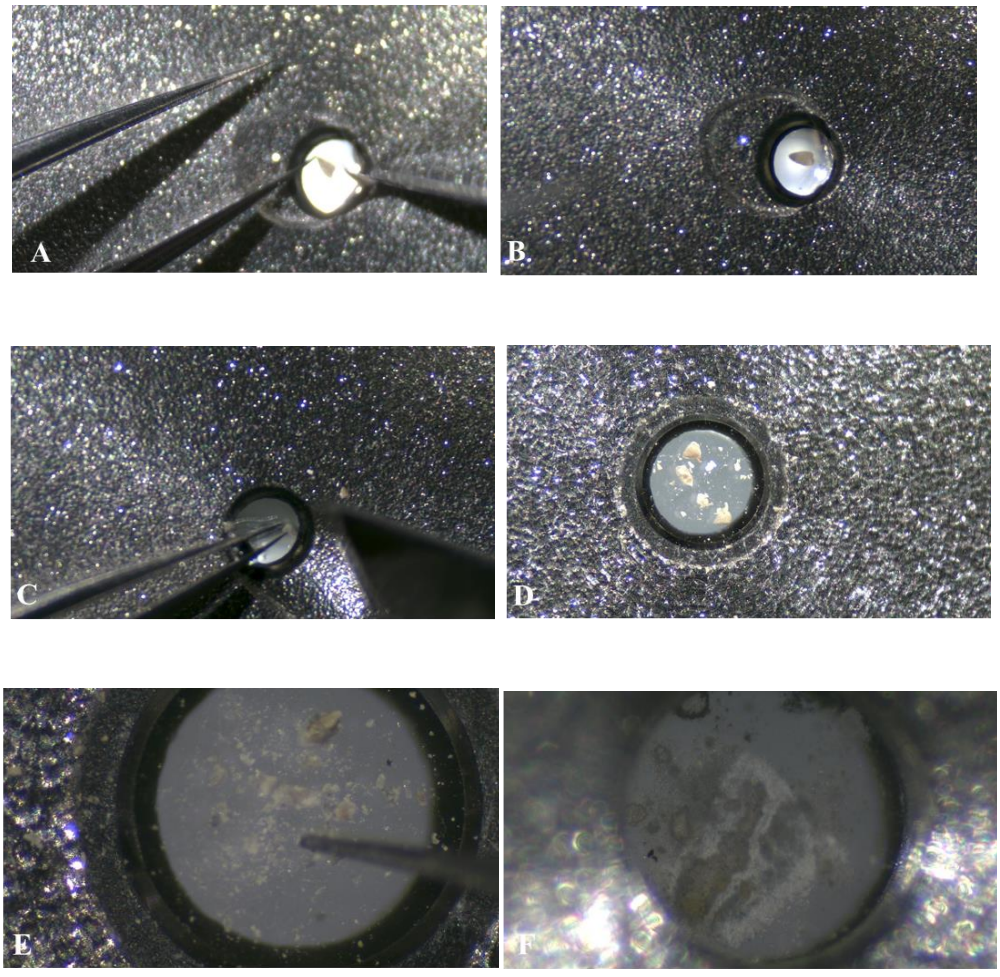

Figure 7. Samples preparation at the synchrotron Diamond cell compression.

4. RESULTS

The December 2020 pilot experiment focused only on the LC_{50}-48 h test and the vitality assessment, to prove whether lethal and sublethal concentrations of synthetic nicotine were responsible of the foraminiferal death.

In April 2021, the previous ecotoxicological test were repeated together with infrared spectroscopy (FTIR) and High Performance Liquid Chromatography (HPLC) analyses carried out after specific developed protocols.

4.1 Foraminiferal LC_{50} tests

4.1.1 December 2020 experiment

The seawater quality parameters (T, S and pH) measured during the December 2020 experiment are reported in the Table 2.

The changes noticed following the LC_{50}-48 h test were minimal compared to the pre-test conditions. Specifically, the temperature and salinity increasing was both uniform in all samples (0.6°C and 1 psu, respectively), while pH decreased at varying intervals in the samples, from a minimum of 0.02 (*T. agglutinans* sublethal R2) to a maximum of 0.10 (*R. globularis* sublethal R3) corresponding to a pH value ranging from 8.33 to 8.31 and from 8.33 to 8.23 respectively.

		T (°C)		S (psu)		pH	
		0 h	48 h	0 h	48 h	0 h	48 h
R.globularis	**CTRL**	22	22.6	35	36	8.34	8.26
	Sublethal R1	22	22.6	35	36	8.32	8.24
	Sublethal R2	22	22.6	35	36	8.34	8.30
	Sublethal R3	22	22.6	35	36	8.33	8.23
	LC_{50} R1	22	22.6	35	36	8.32	8.23
	LC_{50} R2	22	22.6	35	36	8.32	8.27
	LC_{50} R3	22	22.6	35	36	8.33	8.23
Quinqueloculina spp.	**CTRL**	22	22.6	35	36	8.34	8.27
	Sublethal R1	22	22.6	35	36	8.32	8.24
	Sublethal R2	22	22.6	35	36	8.33	8.25
	Sublethal R3	22	22.6	35	36	8.34	8.23
	LC_{50} R1	22	22.6	35	36	8.29	8.23
	LC_{50} R2	22	22.6	35	36	8.31	8.28
	LC_{50} R3	22	22.6	35	36	8.33	8.24
T. agglutinans	**CTRL**	22	22.6	35	36	8.36	8.29
	Sublethal R1	22	22.6	35	36	8.34	8.25
	Sublethal R2	22	22.6	35	36	8.33	8.31
	Sublethal R3	22	22.6	35	36	8.34	8.25
	LC_{50} R1	22	22.6	35	36	8.33	8.24
	LC_{50} R2	22	22.6	35	36	8.32	8.25
	LC_{50} R3	23	22.6	35	36	8.33	8.24

Table 2. Seawater quality parameters measured at the beginning and at the end of the December 2020 experiment. In the table are reported the values for each foraminiferal species, synthetic nicotine concentration and replicate.

The results of the foraminiferal acute toxicity test (LC_{50}-48 h) performed in December 2020 are shown in Table 3. They are expressed as the number of alive individuals for each foraminiferal species after a 48-hour exposure to synthetic nicotine lethal and sublethal concentrations.

Some samples kept all five individuals alive during the test (e.g., *Quinqueloculina* spp. and *T. agglutinans* controls), while in others the number

of live individuals decreased, even to the point of zero (*R. globularis* LC_{50} R1). *Quinqueloculina* spp. was the species with the highest number of individuals remained alive in the samples, while *R. globularis* suffered the greatest decline in viability, with most of its samples containing only 1 live specimen both for lethal and sublethal concentrations.

		R. globularis	***Quinqueloculina* spp.**	***T. agglutinans***
CTRL		3	5	5
Sublethal	R1	1	3	1
	R2	1	5	2
	R3	1	5	2
LC_{50}	R1	0	4	1
	R2	1	2	1
	R3	2	4	1

Table 3. Values of alive foraminiferal individuals after LC_{50}-48 h test performed in December 2020.

The values of Table 3 were then reported as average value for each used concentration and foraminiferal species and converted into viability percentages (Table 4). It might be inferred that, for each taxonomic group, the mortality rate increased as the amount of synthetic nicotine in the samples.

The mortality rate of *R. globularis* grew by 40% for both sublethal and lethal concentrations. Regards *Quinqueloculina* spp., from a total of 100% viability in the control, it dropped to 86% viability in the sublethal concentration and 66% viability in the LC_{50}. For *T. agglutinans*, viability ranged from a total of

100% in the control to 34% in the sublethal concentration and 20% in the lethal one.

% VIABILITY			
	Rosalina globularis	***Quinqueloculina* spp.**	***Textularia agglutinans***
CTRL	60%	100%	100%
Sublethal	20%	87%	34%
LC_{50}	20%	67%	20%

Table 4. Percentages of foraminiferal viability after the LC_{50}-48 h test performed in December 2020.

From the viability percentages, a graph was derived relating the percentages of surviving foraminifera to the concentrations of synthetic nicotine in the experimental samples (Figure 8).

The concentration-response curve revealed that as the concentration of synthetic nicotine in the samples increased, the percentage of alive foraminifera decreased linearly for *Quinqueloculina* spp., while for the other two species (*R. globularis* and *T. agglutinans*), after a significant initial reduction, it tended to stabilise, reaching the 20% at the lethal concentration.

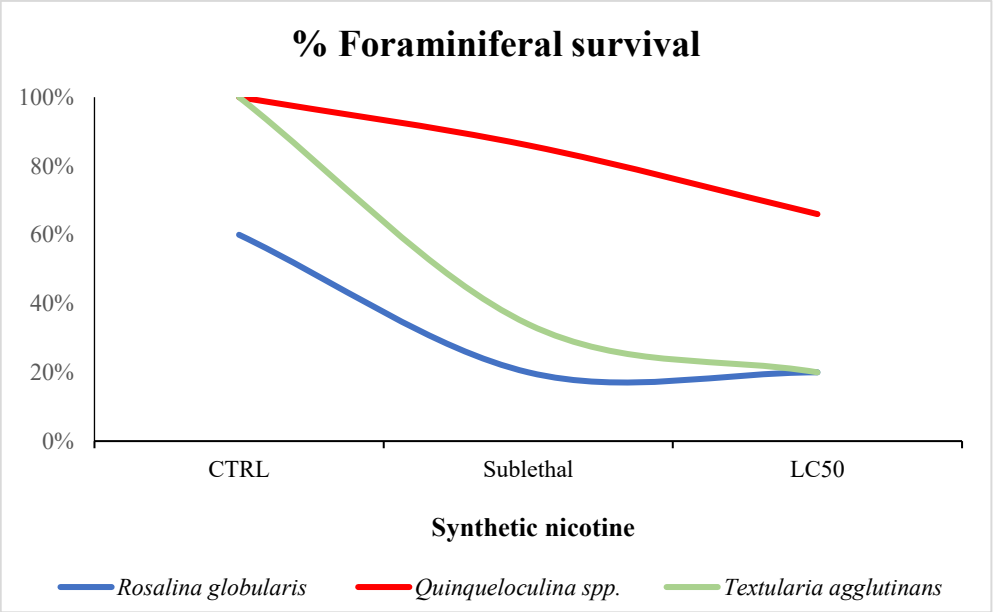

Figure 8. Synthetic nicotine concentrations vs percentage of survived foraminifera (December 2020 LC_{50}-48 h test) for the three studied species: *Rosalina globularis* (blue), *Quinqueloculina* spp. (red) and *Textularia agglutinans* (green).

During the experiment an anomaly was observed. Two of the five individuals of *R. globularis* used as control for the experiment were already dead.

Since the mortality was not caused by the addition of synthetic nicotine but, probably, by an incorrect evaluation of their vitality at the beginning of the experiment, data were modified considering that control sample of *R. globularis* accounted for 3 individuals instead of 5.

In this way, the viability percentage of *R. globularis* control became 100% (Table 5).

% VIABILITY			
	Rosalina globularis	***Quinqueloculina* spp.**	***Textularia agglutinans***
CTRL	100%	100%	100%
Sublethal	20%	87%	34%
LC_{50}	20%	67%	20%

Table 5. Percentages of foraminiferal viability after the LC_{50}-48 h test performed in December 2020. The number of individuals in *R. globularis* control sample was corrected, so the viability of the control became 100%.

Consequently, the concentration-response curve for *R. globularis* also changed: from 100% viability, it dropped to 20% of surviving foraminifera at the sublethal concentration, maintaining this value even at the LC_{50} level (Figure 9).

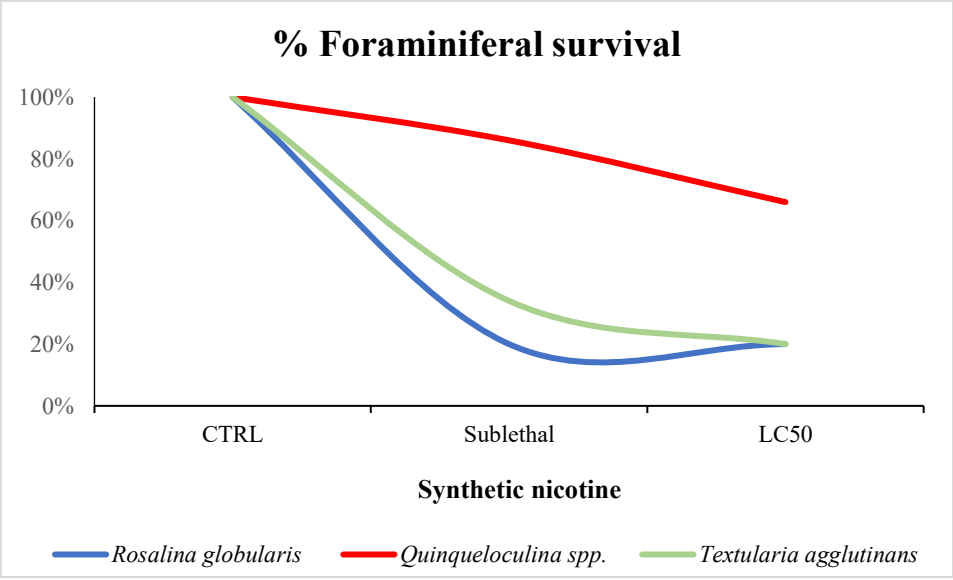

Figure 9. Synthetic nicotine concentrations vs percentage of survived foraminifera (December 2020 LC_{50}-48 h test) for the three studied species, following the change in control sample of *R. globularis*.

The foraminiferal number of each species, counted as dead at the end of the LC_{50}-48 h test, changed after 72-hour CTG recovery. The vitality (not dormancy) in terms of alive specimens was tested by observation of individuals under the epifluorescence microscope and then counted.

During this phase of the experiment, a significant increase in the number of dead individuals was detected in all three species, confirming the total absence of quiescence.

4.1.2 April 2021 experiment

The acute toxicity (LC_{50}-48 h) and vitality tests were also carried out in April 2021, following the same procedures applied in the December 2020 pilot experiment.

The seawater quality parameters (T, S and pH) measured in April 2021 are displayed in Table 6. In all samples, the temperature remained constant before and after the experiment (23°C) and the salinity varied from 36 to 37 psu. Again, pH is the parameter that underwent the most noticeable change, with a minimum decrease of 0.02 from 8.32 to 8.30 (*R. globularis* sublethal R1) and a maximum one of 0.08 from 8.33 to 8.25 (*R.globularis* sublethal R2).

		T (°C)		S (psu)		pH	
		0 h	48 h	0 h	48 h	0 h	48 h
R.globularis	**CTRL**	23	23	35	36-37	8.34	8.32
	Sublethal R1	23	23	35	36	8.32	8.30
	Sublethal R2	23	23	35	36-37	8.33	8.25
	Sublethal R3	23	23	35	36-37	8.33	8.30
	LC_{50} R1	23	23	35	36	8,33	8,30
	LC_{50} R2	23	23	35	36-37	8.33	8.30
	LC_{50} R3	23	23	35	36	8.33	8.30
Quinqueloculina spp.	**CTRL**	23	23	35	37	8.34	8.28
	Sublethal R1	23	23	35	36	8.33	8.28
	Sublethal R2	23	23	35	37	8.33	8.29
	Sublethal R3	23	23	35	36-37	8.32	8.26
	LC_{50} R1	23	23	35	36	8.31	8.25
	LC_{50} R2	23	23	35	36	8.31	8.25
	LC_{50} R3	23	23	35	36	8.32	8.26
T. agglutinans	**CTRL**	23	23	35	37	8.34	8.26
	Sublethal R1	23	23	35	36	8.33	8.26
	Sublethal R2	23	23	35	36	8.33	8.26
	Sublethal R3	23	23	35	36	8.33	8.26
	LC_{50} R1	23	23	35	35	8.32	8.25
	LC_{50} R2	23	23	35	36	8.32	8.26
	LC_{50} R3	23	23	35	36	8.33	8.26

Table 6. Seawater quality parameters measured at the beginning and at the end of the April 2021 experiment. In the table are reported values for each foraminiferal species, concentration, and replicate.

The number of live individuals after the LC_{50}-48 h test conducted in April 2021 was quite heterogenous in the different taxonomic group and samples (Table 7).

Quinqueloculina spp. was again the species with the overall highest number of survived individuals (from 2 in the LC_{50} R2 to 5 in sublethal R3 and LC_{50} R3). *Rosalina globularis* alive individuals ranged from 1 (LC_{50} R2) to 5

(sublethal R3 and LC_{50} R3). *Textularia agglutinans* suffered the greatest decrease in viability, with three of its samples (sublethal R2, LC_{50} R1 and LC_{50} R2) lacking survived individuals.

		R. globularis	***Quinqueloculina* spp.**	***T. agglutinans***
CTRL		4	4	2
Sublethal	R1	3	4	2
	R2	3	4	0
	R3	5	5	3
LC_{50}	R1	2	3	0
	R2	1	2	0
	R3	5	5	3

Table 7. Values of alive foraminiferal individuals after LC_{50}-48 h test performed in April 2021.

Also in the April 2021 experiment, the values were averaged for each lethal, sublethal concentration and foraminiferal species; then converted into viability percentages (Table 8) to construct a graphic (Figure 10) linking the percentages of foraminiferal survival with the concentrations of synthetic nicotine in the samples. To do that the number of living individuals in the control samples was modified as in the previous experiment. This time the anomaly was verified for all the control samples related to the three foraminiferal species.

I reported both the percentage variability considering the real (Table 8) and the corrected (Table 9) values for the control samples.

At sublethal concentration, *Quinqueloculina* spp. retained 80% vitality, while *R. globularis* and *T. agglutinans* viability decreased to 60% and 33% respectively.

The viability of all three species declined at LC_{50} doses, reaching 30% for *R. globularis*, 50% for *Quinqueloculina* spp. and 0% for *T. agglutinans*.

% VIABILITY			
	Rosalina globularis	***Quinqueloculina* spp.**	***Textularia agglutinans***
CTRL	80%	80%	67%
Sublethal	60%	80%	33%
LC_{50}	30%	50%	0%

Table 8. Percentages of foraminiferal viability after the LC_{50}-48 h test performed in April 2021.

In the April 2021 experiment, the concentration-response curves for all three species were very similar, almost parallel to each other. Their slope increases progressively as the amount of synthetic nicotine in the samples increases.

In particular, the *T. agglutinans* curve is a straight line describing a linear relation between the concentration of synthetic nicotine and the foraminifera survival rate.

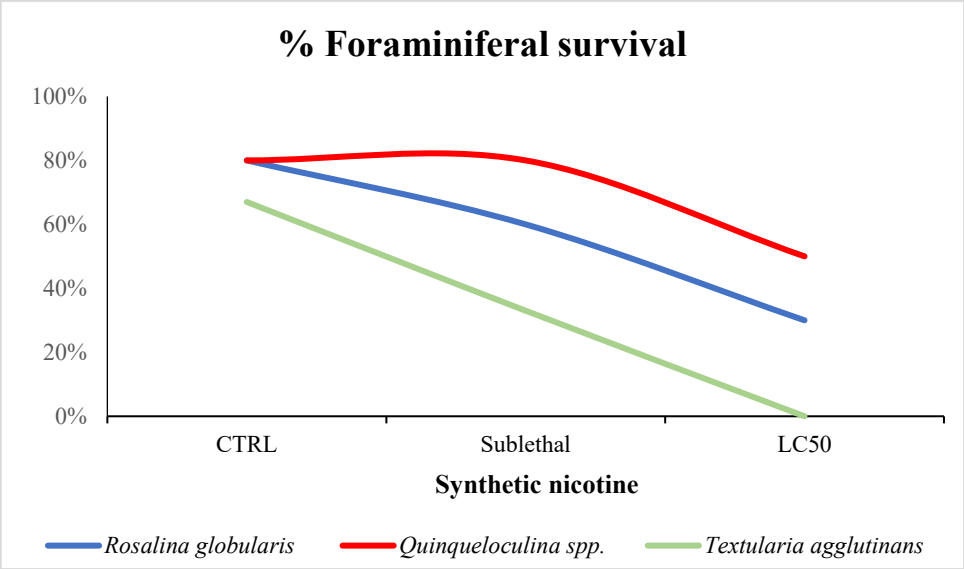

Figure 10. Synthetic nicotine concentrations vs percentage of survived foraminifera (April 2021 LC_{50}-48 h test) for the three studied species: *Rosalina globularis* (blue), *Quinqueloculina* spp. (red), and *Textularia agglutinans* (green).

Table 9 shows the viability percentages considering the corrected values for the controls, which for all three species were converted to 100%.

% VIABILITY			
	Rosalina globularis	***Quinqueloculina* spp.**	***Textularia agglutinans***
CTRL	100%	100%	100%
Sublethal	60%	80%	33%
LC_{50}	30%	50%	0%

Table 9. Percentages of foraminiferal viability with the corrected values for all the three investigated species.

The resulting graphic (Figure 11) is similar to the previous one (Figure 9), but the three curves intersect at the control; it is more evident a linear relation between the concentration of synthetic nicotine and the foraminiferal survival rate.

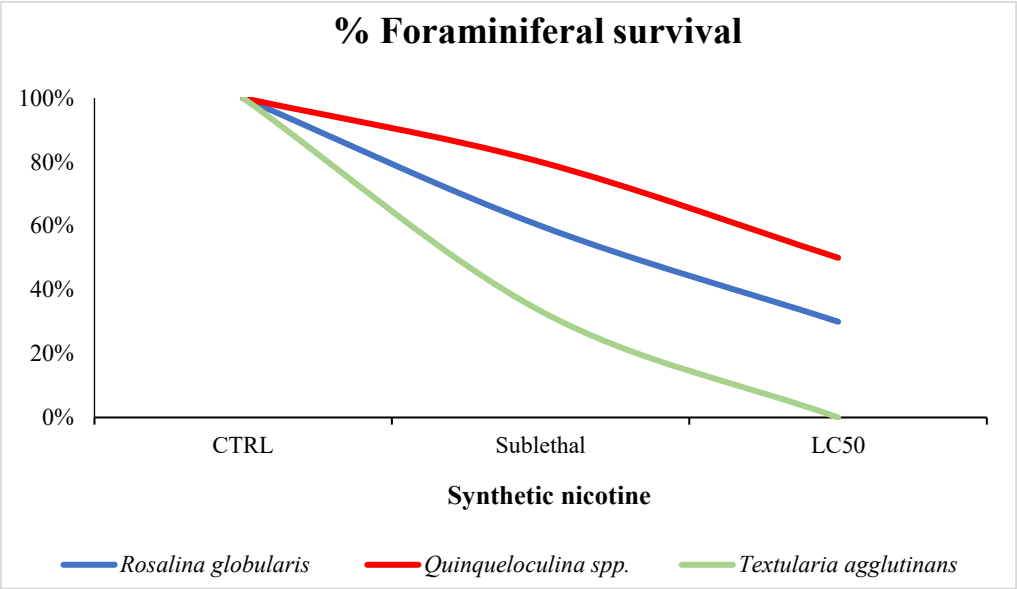

Figure 11. Synthetic nicotine concentrations vs percentage of survived foraminifera for the three studied species, following the change in all the control samples.

During the 72-hour recovery phase, foraminiferal mortality increased drastically, and, as in the December 2020 experiment, no quiescent individuals were identified for any of the three species.

As previously said in the methods, during the April 2021 vitality test some samples (one individual of each control, all sublethal R3 and all LC_{50} R3 samples) were not stained with CTG for the subsequent synchrotron analyses.

4.2 High Performance Liquid Chromatography

For each sample analysed by HPLC a chromatogram was obtained, describing the absorbance (mAu) over time (min) measured at 260 nm.

Utilizing the Mix solutions, the instrument verified that the combination of nicotine (both salt and pure) and cotinine maintained the same absorbance and retention time profile of the three standards (consisting of nicotine salt, pure nicotine and cotinine respectively), whose absorption spectra had been previously identified.

An example of this result is the chromatogram of the Mix 3 + KCl solution (Figure 12), which has two absorption peaks: a smaller one around 10 minutes (corresponding to cotinine) and a higher one around 15 minutes (corresponding to nicotine).

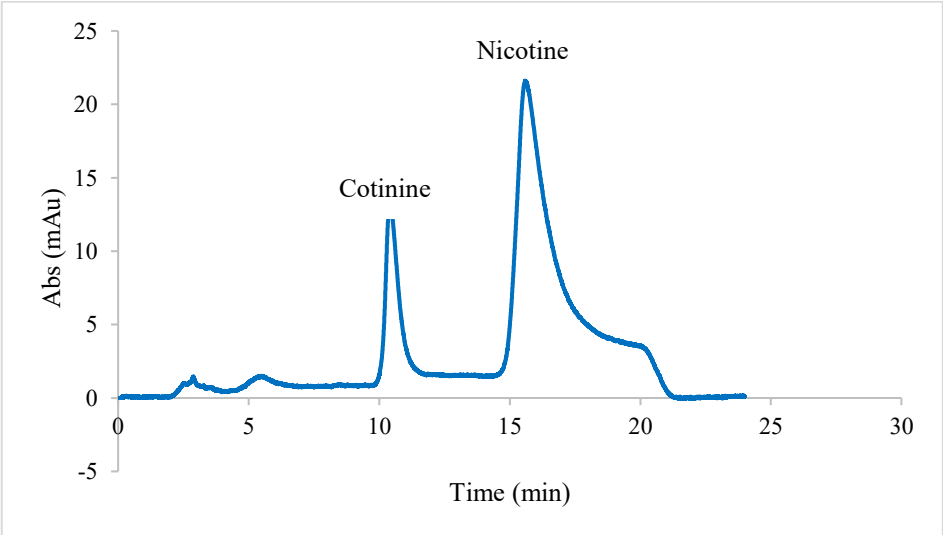

Figure 12. Chromatogram of the Mix 3 + KCl solution.

Chromatograms of all the LC_{50}-48 h test experimental samples showed a very similar pattern for synthetic nicotine, with a maximum absorption peak around 15 minutes, confirming its presence in the solutions in which foraminifera were incubated (except for the controls), while no cotinine peak was detected in any sample.

All data used to estimate the synthetic nicotine recovery rate (N%) for each sample are contained in Table 10 (following the protocol described in the paragraph 3.2.1 of Materials and methods).

Almost all percentages of synthetic nicotine recovery rate were less than 20%.

In all three species control the rate was obviously equal to 0% since the absence of synthetic nicotine.

Textularia agglutinans and *Quinqueloculina* spp. values were similar. *Textularia agglutinans* recovery rates ranged from 10.7% (sublethal R1) to 15.9% (sublethal R2), while in *Quinqueloculina* spp. they changed from 12.9% (sublethal R1) to 16.4% (sublethal R3).

We found the higher variation of synthetic nicotine recovery rate in *R. globularis*, whose sublethal R2 reached 31.8%, whereas the other values were closer to the ones of the other two species, ranging from 13.7% (LC_{50} R1) to 19.3% (LC_{50} R2).

Name	µL Nicotine (HSO_4^-)	Area (mAu)	nmoles	Initial µmoles of synthetic nicotine in solution samples	Final µmoles of synthetic nicotine measured in solution samples	Nicotine recovery rate
T. agglutinans CTRL	0	0	0	0	0	0.0%
T. agglutinans sublethal R1	4.46	743.195	3.40	4.2	0.5	10.7%
T. agglutinans sublethal R2	4.46	1107.947	5.06	4.2	0.7	15.9%
T. agglutinans sublethal R3	4.46	1058.257	4.84	4.2	0.6	15.2%
T. agglutinans LC_{50} R1	12.5	2990.652	13.67	11.9	1.8	15.3%
T. agglutinans LC_{50} R2	12.5	2746.864	12.56	11.9	1.7	14.1%
T. agglutinans LC_{50} R3	12.5	2658.851	12.15	11.9	1.6	13.6%
Quinqueloculina spp. CTRL	0	0	0	0	0	0.0%
Quinqueloculina spp. sublethal R1	4.46	901.549	4.12	4.2	0.5	12,9%
Quinqueloculina spp. sublethal R2	4.46	945.711	4.32	4.2	0.6	13.6%
Quinqueloculina spp. sublethal R3	4.46	1139.925	5.21	4.2	0.7	16.4%
Quinqueloculina spp. LC_{50} R1	16	3509.625	16.04	15.2	2.1	14.0%
Quinqueloculina spp. LC_{50} R2	16	3906.988	17.86	15.2	2.4	15.6%
Quinqueloculina spp. LC_{50} R3	16	3535.302	16.16	15.2	2.2	14.1%
R. globularis CTRL	0	0	0	0	0	0.0%
R. globularis sublethal R1	2.24	641.041	2.93	2.1	0.4	18.3%
R. globularis sublethal R2	2.24	1111.953	5.08	2.1	0.7	31.8%
R. globularis sublethal R3	2.24	595.455	2.72	2.1	0.4	17.0%
R. globularis LC_{50} R1	4.2	1030.853	4.71	4.0	0.6	15.7%
R. globularis LC_{50} R2	4.2	902.317	4.12	4.0	0.5	13.7%
R. globularis LC_{50} R3	4.2	1269.829	5.80	4.0	0.8	19.3%

Table 10. Data used to obtain the synthetic nicotine recovery rate for each acute toxicity test sample (LC_{50}-48 h) of April 2021.

4.3 Fourier Transform Infrared (FTIR) analyses

Data obtained by infrared spectroscopy analyses allowed to assess the synthetic nicotine effects on the biochemical composition of foraminiferal cell and test, focusing on biocalcification processes.

To highlight better the spatial distribution of the biochemical species within the samples, images were presented as RGB assembly, where red represents the protein, green the calcium carbonate and blue is used to represent the chemical distribution of COC (C-glycosidic linkage) bands of carbohydrates.

In this way, cartographies represented the foraminiferal qualitative macromolecular composition by spots of different colours as explained above.

Some cartographies illustrated not broken individuals, others have been elaborated after foraminifera have been crushed by Diamond cell compression.

Figure 13 shows a cartography where are sharply distinguishable calcium carbonate in the test, proteins and carbohydrates in the cytoplasm of a complete individual of *R. globularis* sublethal R3.

In a fragment of the same individual (Figure 14) proteins were still sufficiently recognisable, unlike calcium carbonate and carbohydrates.

The Figure 15 cartography displayed a specimen of *Quinqueloculina* spp. (LC_{50} R3); the oldest chambers, where green is visible, had still calcium carbonate, while the youngest ones coloured in blue and red had probably lost most of the calcitic test; proteins and carbohydrates were present.

In a fragment (sublethal R3) and a whole individual (control) of *T. agglutinans* cartographies, the three macromolecules spots appeared uniformly distributed; this made it difficult to distinguish the shell composition from the cellular one in the whole individual (Figures 16 and 17).

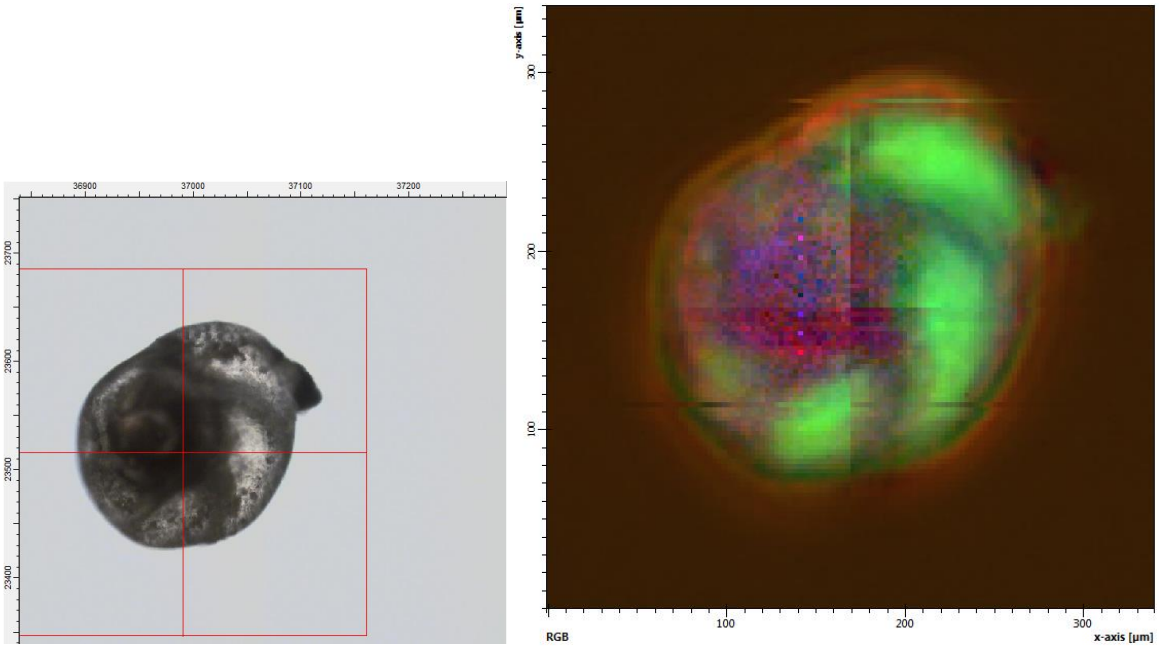

Figure 13. Cartography of an entire specimen of *R. globularis* from sublethal R3 sample.

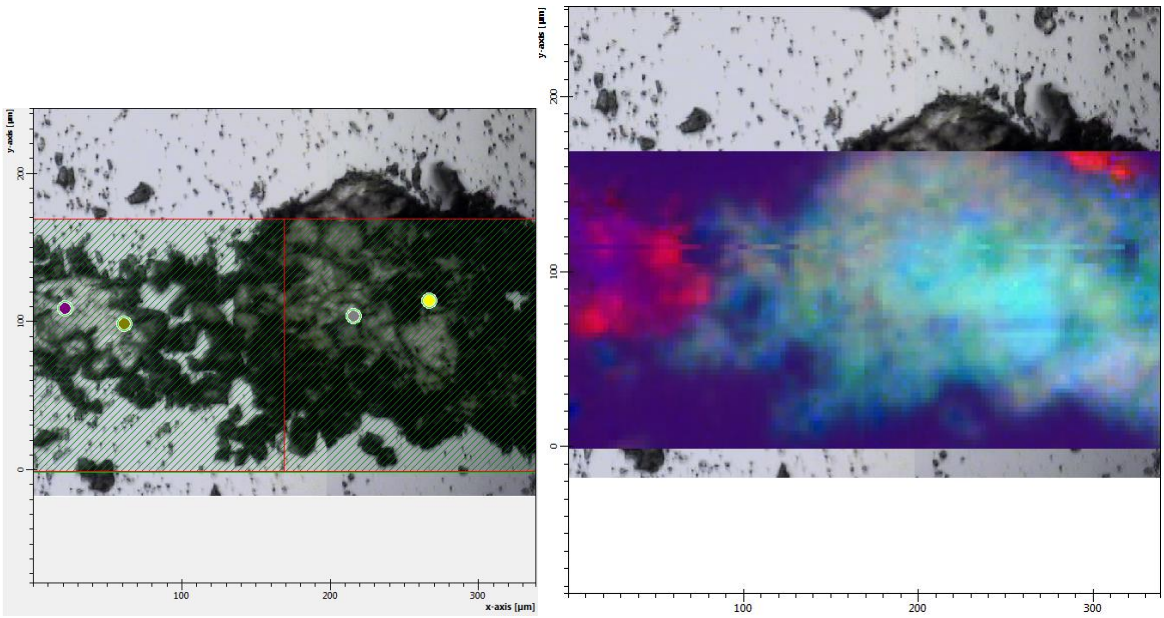

Figure 14. Cartography of a fragment of *R. globularis* from sublethal R3 sample.

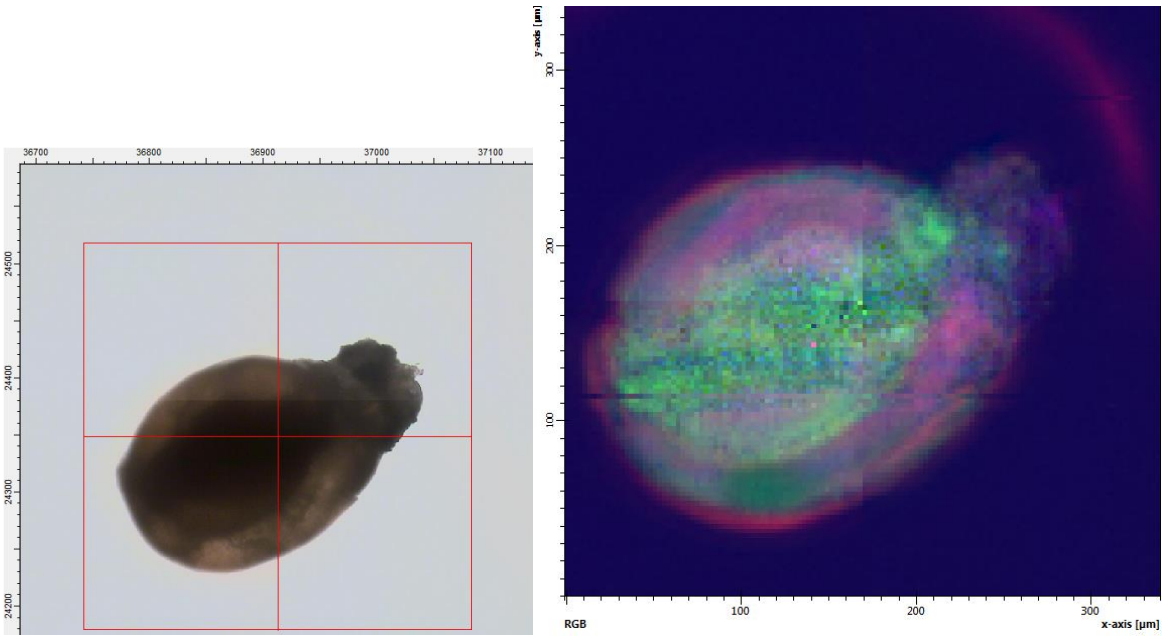

Figure 15. Cartography of *Quinqueloculina* spp. specimen from LC_{50} R3 sample.

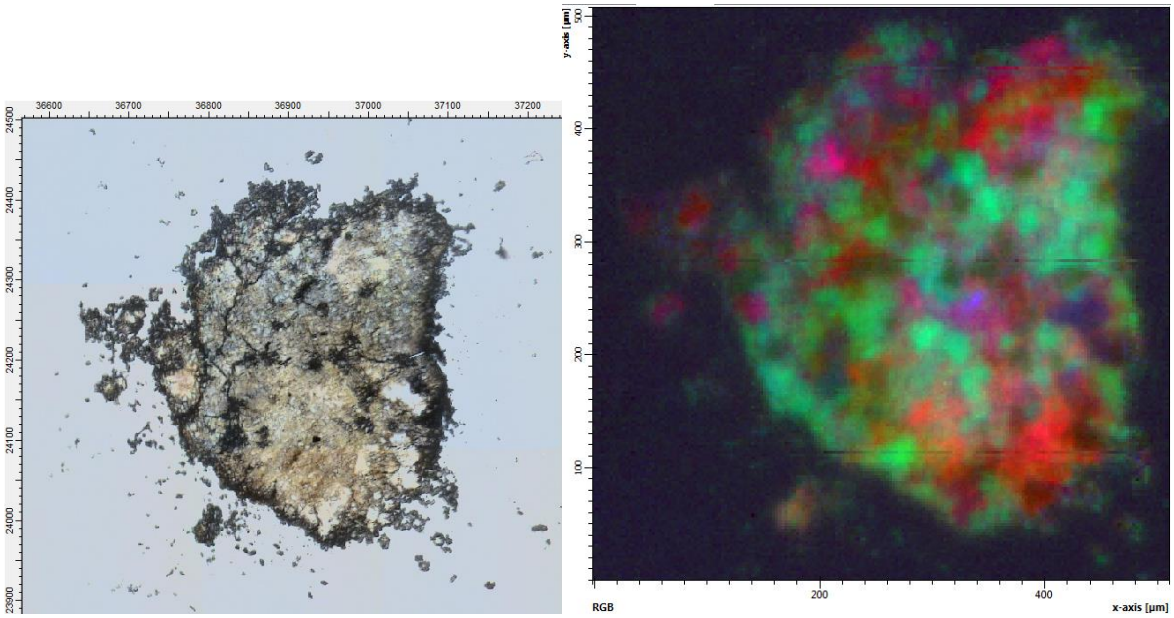

Figure 16. Cartography of a fragment of *T. agglutinans* from sublethal R3 sample.

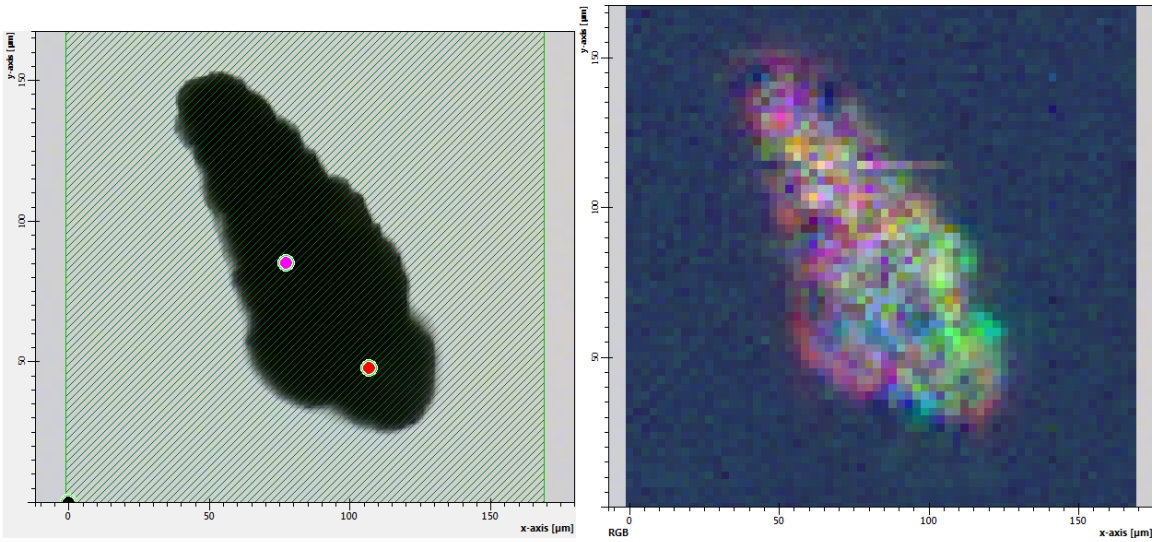

Figure 17. Cartography of an entire specimen of *T. agglutinans* from the control sample.

To evaluate the nicotine effect on foraminifera, band integrals were calculated: 1700-1605 cm^{-1} for proteins, representative of cytoplasm, 3000-

2800 cm^{-1} for lipids, 2660-2435 cm^{-1} overtone 1850-1765 cm^{-1} for calcium carbonate and 1200-950 cm^{-1} for phosphates, silicates, and carbohydrates. Results of the band's integrations processes were calculated in Quasar (https:\\quasar.codes), the outlier values were removed, and then averaged for every treatment in order to allow for comparison. Integrals were analyzed with one-way ANOVA and plotted in Origin (Origin labs). Average spectra were calculated in Quasar, and two PCAs were performed: one on vector normalized whole spectral range and the second on vector normalized 2^{nd} derivative Amide I (1700-1600 cm^{-1}). Results of PCAs have been plotted using Origin (Origin labs) (Figures 22 and 23).

Fourier Transform Infrared (FTIR) data are shown in the following graphics, which were only obtained for *T. agglutinans* and *R. globularis*, as just one individual of *Quinqueloculina* spp. was analysed at the synchrotron.

Figure 18 displays the average spectra of all *T. agglutinans* (18A) and *R. globularis* (18B) analysed samples (control, sublethal, and LC_{50}).

The sublethal and LC_{50} spectra of *T.agglutinans* (Fig. 16A) had a different trend, as can be observed from the different height of the blue peak (sublethal) and the red peak (LC_{50}) in the range of phosphates, silicates and carbohydrates (1000-1200 cm^{-1}) as indicated by the arrow in the figure 18A.

This variation was not found in *R. globularis* (Fig.18B), but in this species was present a difference between the sublethal (blue peak) and LC_{50} (read peak) averaged spectra corresponding to the range of cytoplasmatic proteins (1700-1605 cm^{-1}) as indicated by the arrow. The protein signal of the sublethal spectrum was less evident.

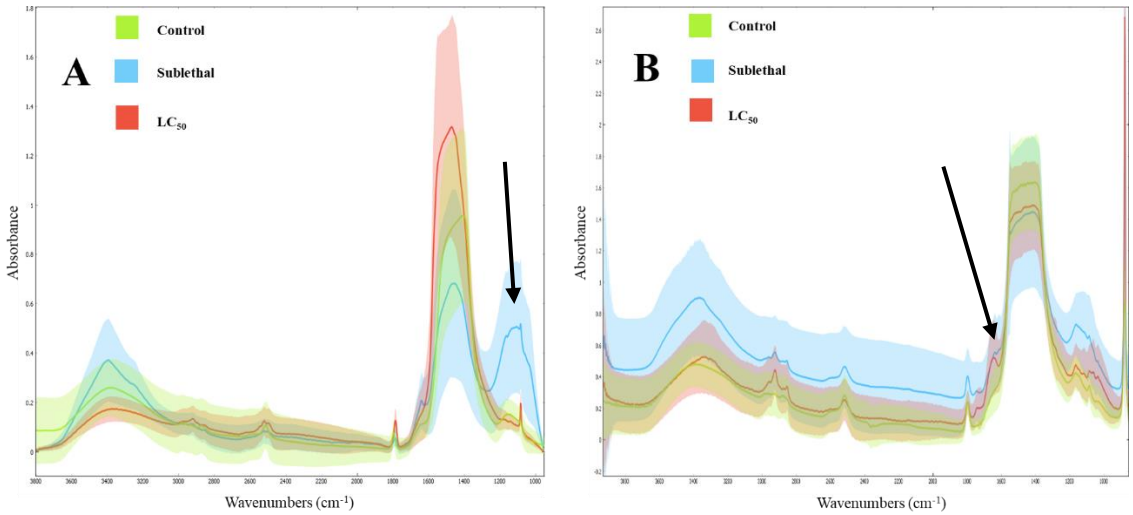

Figure 18. Average spectra of all *T. agglutinans* (A) and *R. globularis* (B) analysed samples.

Considering only the spectra of the sublethal (blue peak) and LC_{50} (red peak) concentrations, the latter had fewer proteins than the sublethal in *T. agglutinans*, as evidenced by the absence of the red peak in the range of 1600-1800 cm^{-1} (Figure 19A arrow). In contrast, the LC_{50} of *R. globularis* has a slightly higher protein content than the sublethal, in fact the red peak is higher than the blue one (Figure 19B arrow).

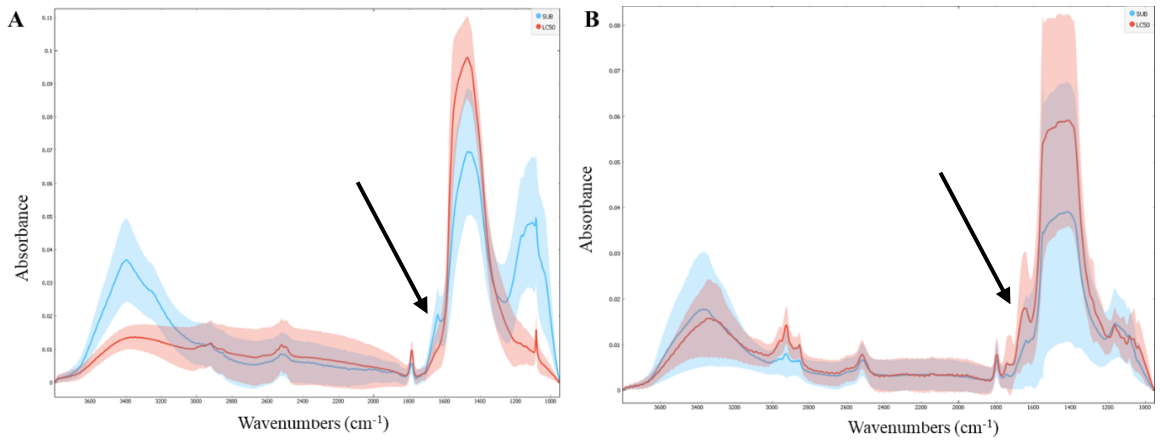

Figure 19. Sublethal and LC_{50} average spectra of *T. agglutinans* (A) and *R. globularis* (B)

Figures 20 and 21 represent histograms of selected integral band ratios for sublethal and LC_{50} samples of both species.

Band integrals on proteins and lipids can give information of the status of the organic content of the foraminifera, in terms of cytoplasm average composition. The band of calcium carbonate and the one of phosphates/carbohydrates (also comprehending a signal from chitin), can provide more information about the shell composition. The variations of the key macromolecules composing the foraminifera were here presented normalized to the protein content, in order to remove any bias due to the difference of thickness within the population of the inspected samples.

Textularia agglutinans LC_{50} samples had more calcium carbonate/proteins and carbohydrates/proteins ratios than sublethal (20A-20C) ones. Conversely, sublethal had a higher lipids/proteins ratio than LC_{50} concentration (20B).

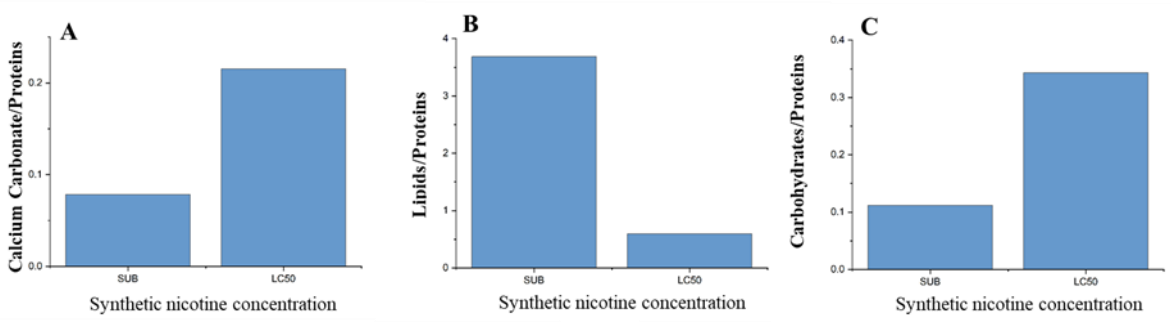

Figure 20. Histograms of the ratios Calcium carbonate/proteins, Lipids/Proteins and Carbohydrates/proteins for *T. agglutinans* sublethal and LC_{50} samples.

At the contrary of *T. agglutinans* trend, *R. globularis* sublethal samples had a higher calcium carbonate/proteins and carbohydrates/proteins content than the LC_{50} samples (21A and 21C). LC_{50} sample had instead a slightly higher lipids/proteins ratio than the sublethal sample (21B).

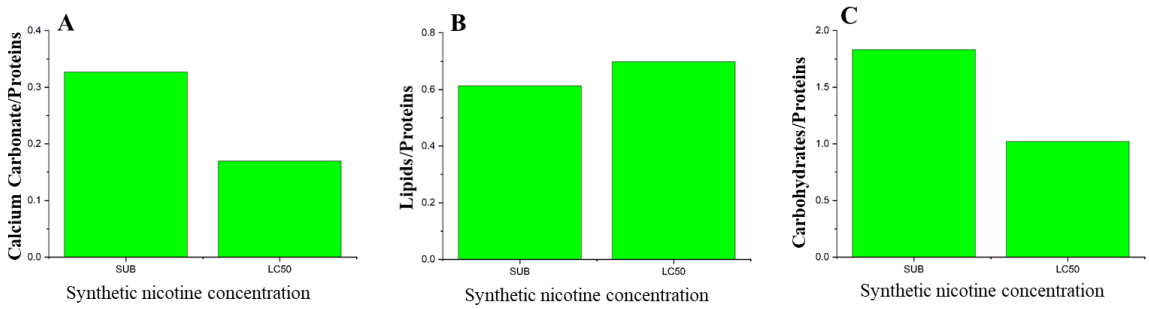

Figure 21. Histograms of the ratios Calcium carbonate/proteins, Lipids/Proteins and Carbohydrates/proteins for *R. globularis* sublethal and LC_{50} samples.

Figure 22 shows the two PCAs of *T. agglutinans*. Graphics 22A and 22B refer to the PCA of the complete spectral range of this species.

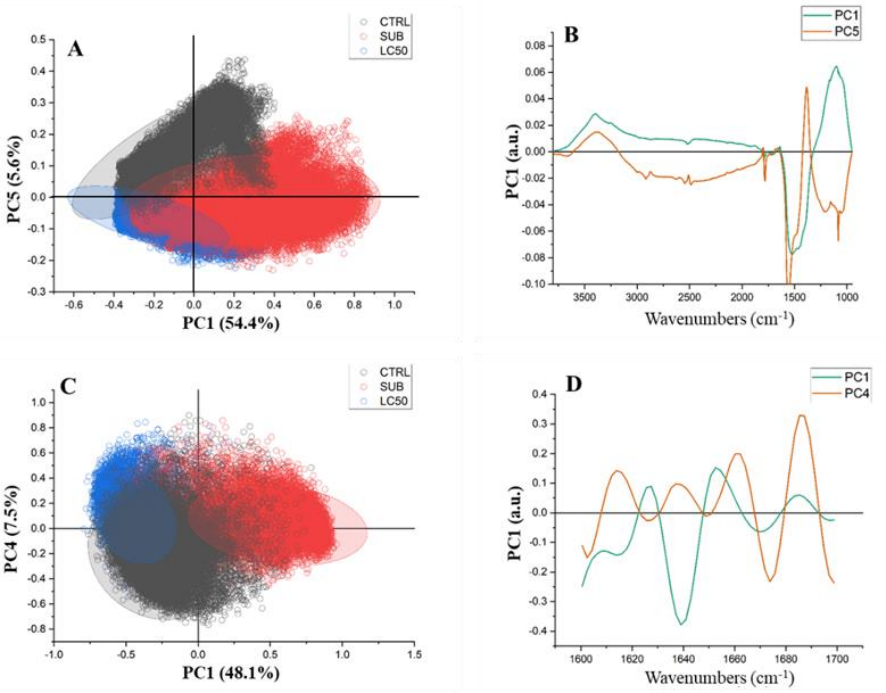

Figure 22. PCAs of *T. agglutinans*

Each analysed sample (control, sublethal and LC_{50}) had a distinct cluster. Between control (black) and LC_{50} (blue), there was a significant difference in proteins, which decreased in LC_{50} (22A). In the graphic 22B, this change corresponded to the difference between the PC1 peak (green) and PC5 peak (orange) at the about 1500 cm^{-1} wavelength.

The sublethal (red), on the other hand, deviated from both control and LC_{50} for phosphates, silicates and carbohydrates (22A); this corresponds to the PC1 and PC5 peaks at about 1000 cm^{-1} wavelength (22B).

Graphics 22C and 22D focused on *T. agglutinans* proteins (zoom between 1600 and 1700 cm^{-1} wavelength). In particular, the PC1 peak (green) at 1640 cm^{-1} is linked to a disorder in the secondary structure of LC_{50} proteins.

Figure 23 shows the two *R. globularis* PCAs. Unlike *T. agglutinans*, in *R. globularis* there was no clear distinction in macromolecular composition between control, sublethal and LC_{50}. As previously illustrated (Figures 19B and 21), the sublethal sample had the highest macromolecular variability; indeed, in the graphic 23A, its cluster (red) also includes the control (black) and the LC_{50} (blue) ones.

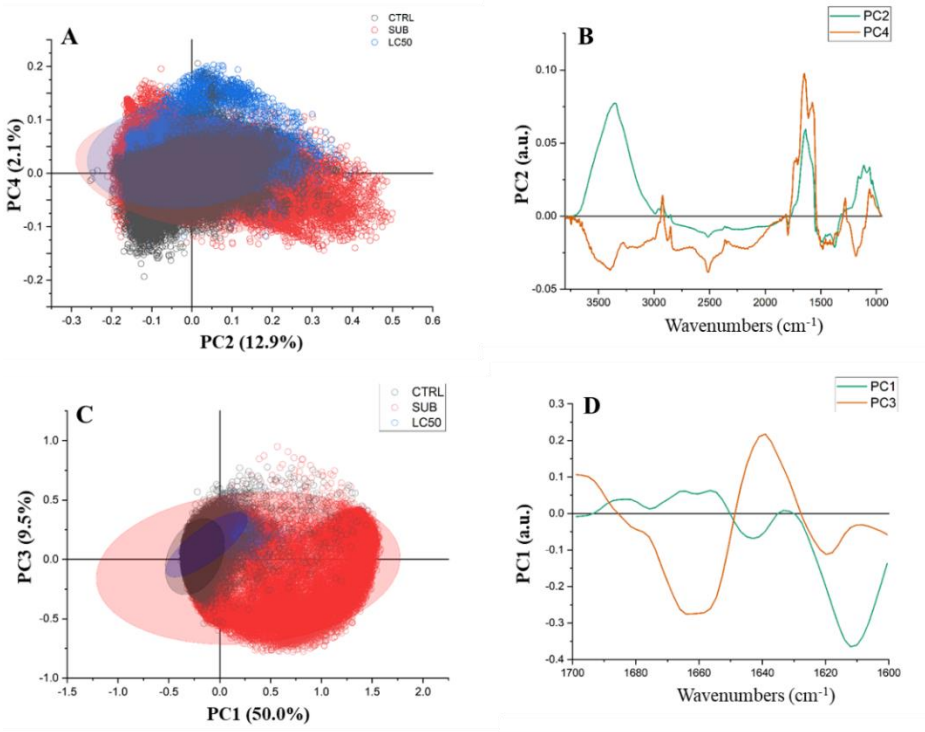

Figure 23. PCAs of *R. globularis*

The histograms in the Figure 24 refer to the total lipid content, expressed as CH_2-CH_3 mean integral, for each sample of *T. agglutinans* (24A) and *R. globularis* (24B). In both species treated with the LC_{50} concentration there was a higher lipid content than the control and the sublethal treatment.

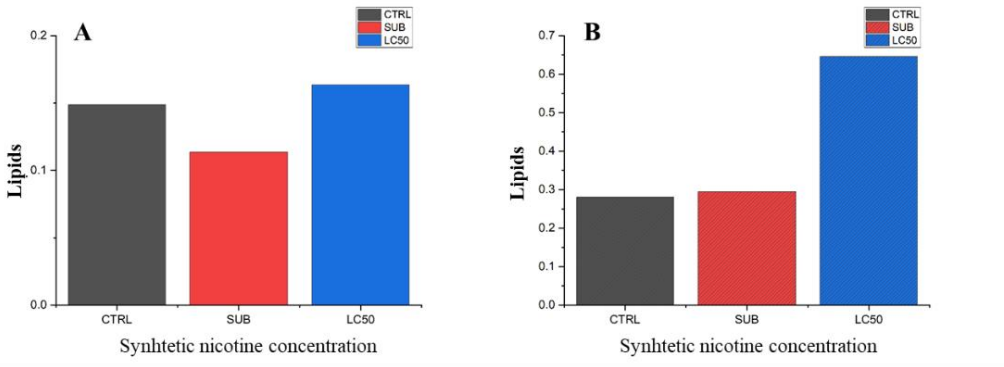

Figure 24. Total lipid content comparison charts for *T. agglutinans* (A) and *R. globularis* (B)

Fourier Transform Infrared (FTIR) data are finally represented as histograms of selected integral band ratios for all samples (control, sublethal, and LC_{50}) of the two species (Figures 25 e 26). As in Figures 20 and 21, the variations of macromolecules have been normalized to the protein content, to remove any bias due to the difference of thickness within the population of the inspected samples.

Both species, in a different way, were affected by the pollution of synthetic nicotine. In the case of *T. agglutinans* (Figure 25), it was possible to observe that the macromolecules constituting the individuals behaved differently. The

values for the control and LC_{50} samples respectively were similar for all studied ratios; but the content in lipids/proteins was a bit higher (Figure 25A) and the calcium carbonate/proteins value was lower (Figure 25B) for the lethal concentration of synthetic nicotine.

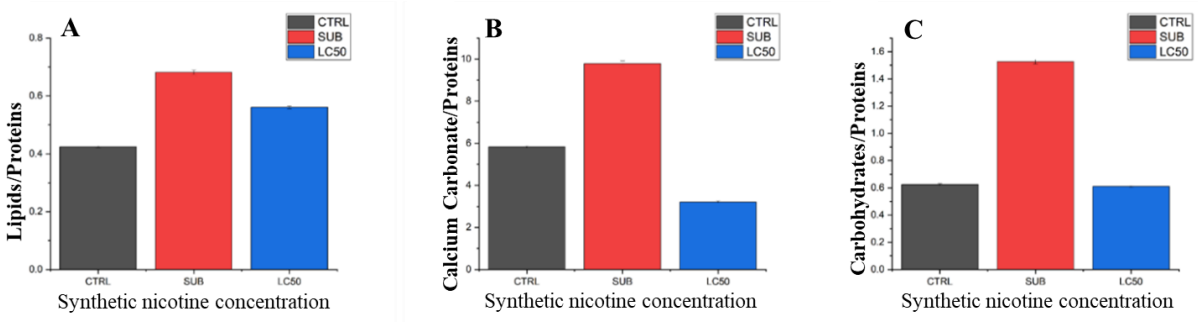

Figure 25. Histograms of the ratios Lipids/proteins, Calcium carbonate/proteins and Carbohydrates/proteins for all samples of *T. agglutinans*.

Conversely, *T. agglutinans* incubated with a sublethal concentration of synthetic nicotine behaved differently; it seems that the pollutant caused the cellule to respond with an increase in protein synthesis linked to a contemporary increase in the carbohydrates/silicates signal. Considering only the signal of carbonates (data not shown), it was possible to describe a decrease of it in both lethal and sublethal synthetic nicotine concentrations.

As *T. agglutinans*, *R. globularis* showed similar values for the control and LC_{50} synthetic nicotine concentration relating to all macromolecular setting, with a bit higher concentration of lipids/proteins (Figure 26A) and a lower

calcium carbonate/proteins content (Figure 26B) for the lethal concentration of synthetic nicotine.

However, sublethal concentrations of synthetic nicotine reduce protein synthesis in individuals of *R. globularis*, resulting in increased lipid, calcium carbonate and carbonate/silicate signals.

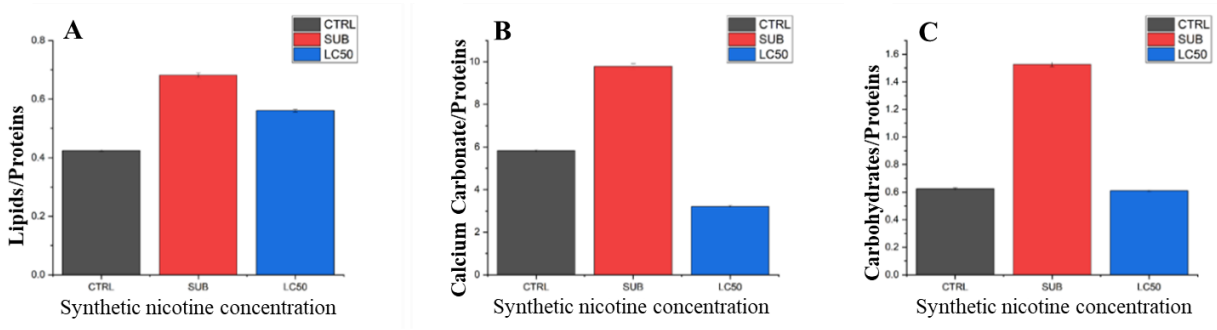

Figure 26. Histograms of the ratios Lipids/proteins, Calcium carbonate/proteins and Carbohydrates/proteins for all samples of *R. globularis*.

5. DISCUSSIONS

The overall work carried out for this master's degree thesis was the evaluation of the impact of synthetic nicotine, the main component of a specific emerging pollutant, the cigarette butt, on three different species of benthic foraminifera. Each of the three species belongs to a different taxonomic group among the foraminifera and they identify the three different ways in which these organisms build their shells. *Rosalina globularis* secretes a perforated or hyaline calcium carbonate test; *Quinqueloculina* spp. specimens biocalcify in the same way, but their shell has no pores, so it is imperforate or porcelaneous; finally, *T. agglutinans* agglutinates particles of various mineral and organic types found in the sediment where it lives using a calcium carbonate cement.

The first step involved the development and implementation of a protocol to perform an acute toxicity test (LC_{50}-48 h) aimed at detecting the direct effect of synthetic nicotine on the viability and biomineralization processes of the three studied foraminiferal species. The second stage involved the analysis, by HPLC, of the solutions in which foraminifera were incubated during the LC_{50}-48 h test, to detect the presence of synthetic nicotine and cotinine (a primary product of nicotine metabolism) as possible biomarkers associated with exposure to cigarette butts.

For the first phase, two LC_{50}-48 h tests were conducted at different times (December 2020 and April 2021); both confirmed that synthetic nicotine is acutely toxic at the different concentrations considered (lethal and sublethal) to all three foraminiferal species.

In detail, observing the relative graphics with the viability values (Figures 27A-27B) it is deducible that *Quinqueloculina* spp. was the most resistant group in both tests, while *R. globularis* and *T. agglutinans* were the most sensitive species in December 2020 and April 2021 tests, respectively.

The LC_{50}-48 h test performed by Caridi et al. (2020) with CB leachate had a different outcome. As shown in Figure 27C, *T. agglutinans* was the most resistant species, while the two calcareous species, particularly *R. globularis*, were the most sensitive.

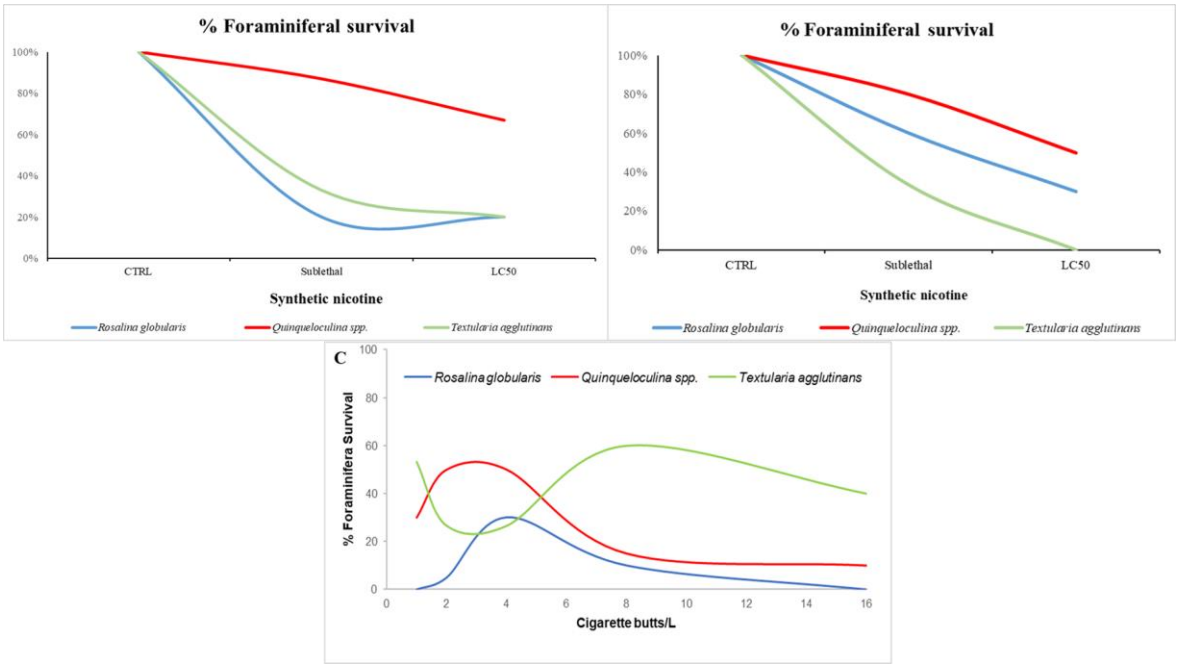

Figure 27. Synthetic nicotine concentrations vs percentage of survived foraminifera for the three studied species: *Rosalina globularis* (blue), *Quinqueloculina* spp. (red) and *Textularia agglutinans* (green): A) December 2020 LC_{50}-48 h test; B) April 2021 LC_{50}-48 h test; C) LC_{50}-48 h test performed by Caridi et al. (2020)

Considering the variability of the results obtained in the three different acute toxicity tests, there is not the same species-specific and biomineralization-dependent response depending on whether the acute toxicity test is conducted with synthetic nicotine or leachate. However, it is clear that different species, based on their biomineralization mechanism, are sensitive to lethal and sublethal concentrations of the pollutant, whether represented by the cigarette butt or by its dominant content, nicotine.

In fact, there is a definite mortality rate in all three species, at lethal and sublethal concentrations, with both CB leachate and synthetic nicotine. Moreover, in both situations, one species achieved 100% mortality: *T.*

agglutinans in the April 2021 test with synthetic nicotine and *R. globularis* with CB leachate (Caridi et al., 2020).

As for the second stage of evaluation of synthetic nicotine in the culture medium, the recovery rate of synthetic nicotine in the solution as measured by HPLC, ranged from 11% to 32% (excluding controls). This suggests that the foraminifera have absorbed the remaining synthetic nicotine, at least to a large extent, roughly between 89% and 68%. These high percentages suggest that the cause of foraminiferal death is primarily related to the presence of this pollutant. However, the possibility that a small amount of synthetic nicotine may have remained attached to the walls of the jars containing the foraminifera or may have been lost during the process of 'washing' cannot be ruled out. This step is related to the cleaning of foraminiferal samples with filtered seawater in order to remove any remaining CTG or other material before the observation under an epifluorescence microscope.

No traces of cotinine were found in the growth medium using HPLC; it is likely that foraminifera, being unicellular eukaryotic organisms, are unable to convert nicotine into its metabolite cotinine as they lack nicotine acetylcholine receptors (nAChRs) or their homologues (Cecchini and Chageux, 2015); alternatively, this process takes longer than 48 hours (experiments time) for these organisms.

There are no data in literature reporting the presence of cotinine in microorganisms (Micevska et al., 2006; Parker and Rayburn, 2017; Bonanomi et al., 2020; Quéméneur et al., 2020), apart from the works of Wright et al. (2015) and Chang et al. (2015) that assess the bioaccumulation of cotinine in metazoans.

The results of both experimental phases (LC_{50}-48 h acute toxicity tests and HPLC analysis of the culture medium) allowed us to hypothesise the involvement of synthetic nicotine as the primary driver for the mortality and decalcification of foraminiferal shells. In particular, *R. globularis* and *T. agglutinans* were the species that underwent the greatest decalcification effect, while *Quinqueloculina* spp. was the species that underwent this process least.

The reason may be the different biomineralization mechanisms characterising the three species. *Quinqueloculina* spp. is a miliolid whose calcium carbonate shell is imperforate (de Noojer et al., 2008; de Noojer et al., 2009; Zamora-Duran et al., 2020); the test wall has no pores and is made up of crystals of the same mineral arranged in a continuous manner to form a single thick layer that probably limits the passage of synthetic nicotine, acting as a more efficient barrier than *R. globularis* and *T. agglutinans* tests.

Rosalina globularis, like *Quinqueloculina* spp., is a calcareous species, but

monolamellar and perforate; the test consists of a calcite lamella and pores running through the entire thickness of the shell wall (Erez et al., 2003; de Noojer et al., 2014). Because of this, the presence of channels and the reduced thickness of the shell, it can be assumed that synthetic nicotine is easily absorbed through the foraminiferal test.

Textularia agglutinans, as an agglutinated species, only secretes calcium carbonate cement which it uses as a glue for sediment granules and other material lining the cell of the organism. Synthetic nicotine may have had a more rapid effect on the decalcification of the cement, resulting in the breakdown of the agglutinating shell and increased uptake by the cell.

The general hypothesis is that the test acts as a barrier, and depending on the biomineralization pattern of the species, it may undergo more or less different decalcification processes; similarly, the foraminiferal cell is more or less vulnerable to lethal and sublethal concentrations of synthetic nicotine. It must be emphasised, however, that decalcification of the shell does not necessarily correspond to the death of the individual.

In fact, as can be seen in Figure 28 showing the three species of foraminifera before and after the LC_{50}-48 h test in April 2021, although some organisms died during the experiment (Figures 28B-28D), shell decalcification is not

visually perceptible. In contrast, in the experiment by Caridi et al. (2020), shell dissolution is clearly visible in all three species due to CB leachate.

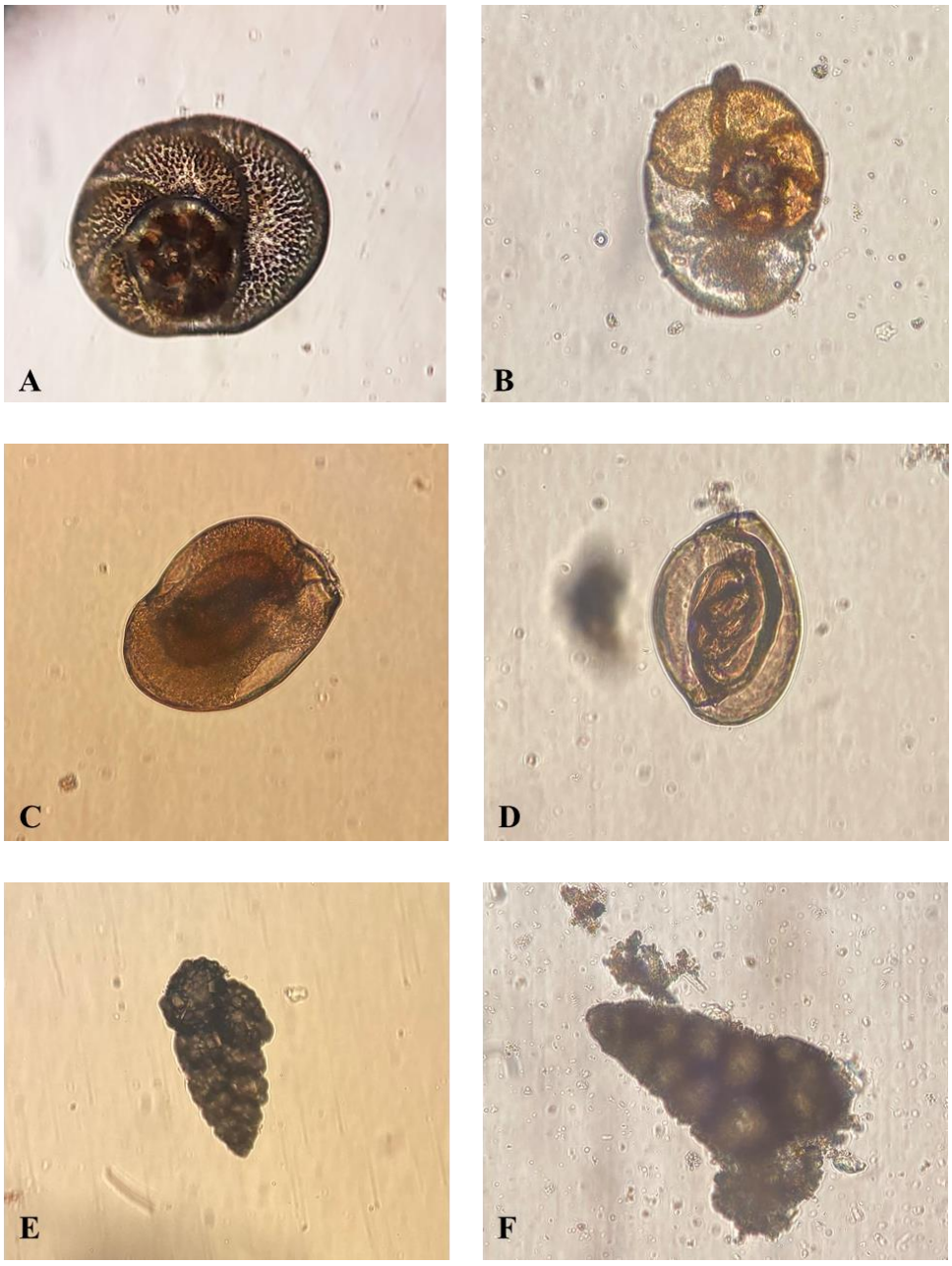

Figure 28. Foraminiferal species before (A, C, E) and after (B, D, F) the April 2021 LC_{50}-48 h test observed under the optical microscope. The species are: *Rosalina globularis* (A, B); *Quinqueloculina spp*. (C, D); *Textularia agglutinans* (E, F).

This suggests that CB leachate produces a major test decalcification of the three foraminiferal species than synthetic nicotine alone, probably due to the presence of more toxic substances in the culture medium. The combination of substances contained in the CB leachate is, indeed, responsible for a higher pH decrease in the culture medium than synthetic nicotine, thus supporting a more rapid and intense dissolution of the calcium carbonate in the shell of the three foraminiferal species.

Specifically, in the LC_{50}-48 h tests performed with synthetic nicotine, the pH varied from a minimum of 0.02 (*T. agglutinans* sublethal R2) to a maximum of 0.10 (*R. globularis* R3) in the December 2020 test, and from a minimum of 0.02 (*R. globularis* sublethal R3) to a maximum of 0.08 (*R. globularis* sublethal R2) in the April 2021 test; in the test performed by Caridi et al. (2020), however, the pH displayed a progressive decrease with increasing cigarette butt concentration, ranging from 0.03 (*R. globularis* R3, 1 cigarette butt/L) to 0.78 (*T. agglutinans* R1, 8 cigarette butts/L).

The phase following the acute toxicity tests (LC_{50}-48 h) and the HPLC analysis of the culture medium focused on synchrotron (FTIR) analyses, in which the effects of synthetic nicotine on the foraminifera shell and cell were examined in detail.

The results of FTIR analyses revealed similar effects of synthetic nicotine on

both the shell and the cell. In particular, the only two species that could be analysed using FTIR, *T. agglutinans* and *R. globularis*, revealed different behaviours, in response to the synthetic nicotine pollution, on their tests and shell-associated organic matrix.

For *T. agglutinans*, specimens subjected to the lethal concentration (LC_{50}) show a higher calcium carbonate content (cement) in the test and fewer carbohydrates (both data normalised to the protein content), interpreted as polysaccharides of a chitinous or pseudo-chitinous origin that constitute the organic matrix of the foraminiferal shell (Loeblich and Tappan, 1964; Banner et al., 1973; Traverse, 2007); the trend is opposite for individuals treated with the sublethal concentration (Figure 29).

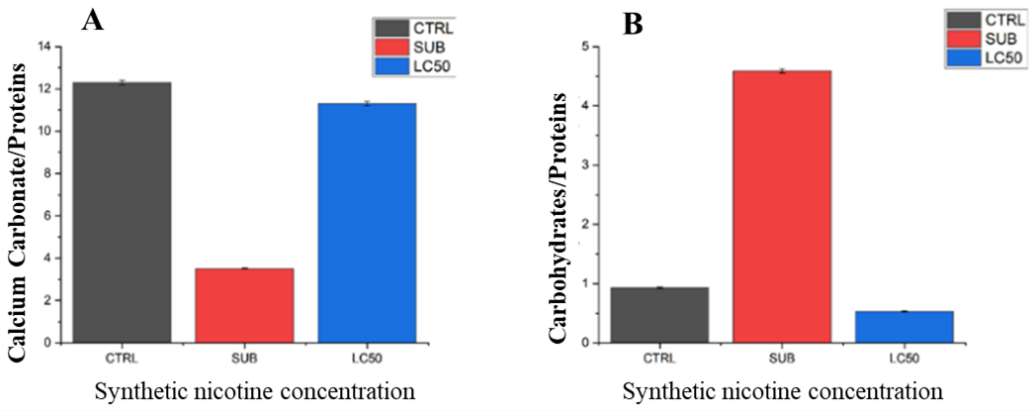

Figure 29. Histograms of the Calcium carbonate/proteins and Carbohydrates/proteins ratios for all samples of *T. agglutinans*.

The lethal dose probably caused damage to the shell organic matrix by reducing its polysaccharide component. The organic matrix of the shell can be

defined as organic foraminiferal linings and identified as a structural component of complete foraminiferal tests consisting of mineral and organic components. According to Hottinger (2006), organic lining itself represents an organic cell envelope constructed from mucopolysaccharides, located between the plasmalemma (cell membrane) and the biomineralized or agglutinated test (Figure 30). Hottinger (2006) recommended the organic lining (proposed by Loeblich and Tappan, 1988) in favour of Inner Organic Lining (IOL) introduced by Anderson and Bé (1978a).

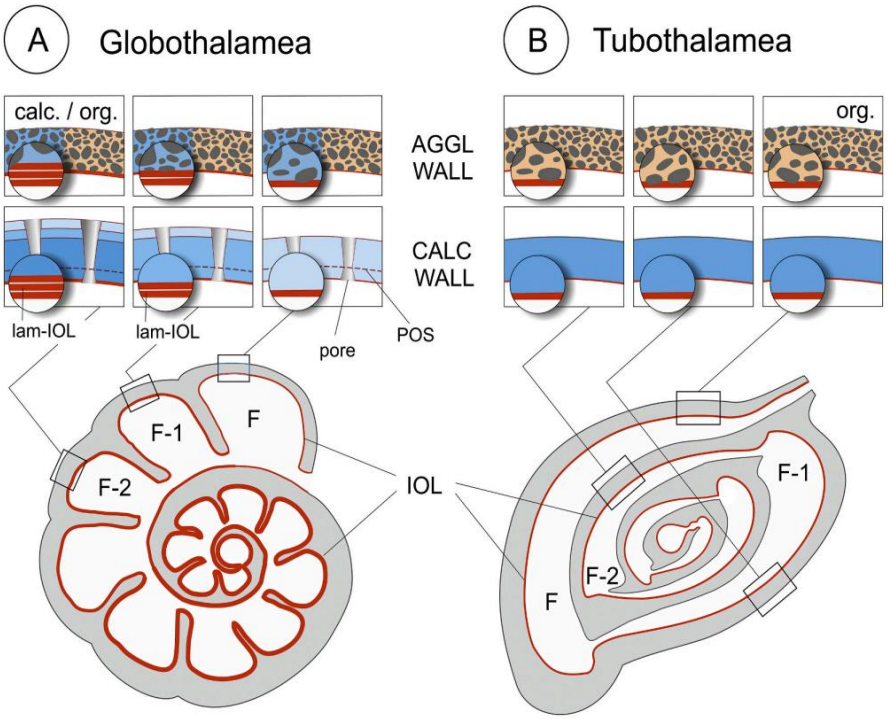

Figure 30. Inner Organic Lining (IOL) identified in cross-section of globothalamen and tubothalamen foraminiferal tests. Three final (distal) chambers are labelled from (F) to (F-2) to present schematic close-ups of their either agglutinated or calcareous walls. Globothalamean IOL tends to be thicker and laminated in earlier chambers in contrast to tubothalamean one which is thinner and nonlamellar. Agglutinated globothalamean tests are composed of foreign mineral grains cemented by organic (org.) and/or calcareous (calc.) matter. (Tyska et al., 2021)

From the results, therefore, it could be hypothesised that the reduction in the polysaccharide component of the IOL induced the cell to produce more calcium carbonate cement to preserve the test strength and defend the cell. This strategy was not adopted by *T. agglutinans* individuals subjected to the sublethal concentration of synthetic nicotine; in this case, more dissolution of the calcium carbonate cement probably occurred with an increase in the IOL polysaccharides. This is confirmed in the overall wavelength spectrum by the difference between the sublethal peak (blue) and the LC_{50} peak (red) in the range 1000-1200 cm^{-1} (circled in Figure 31), corresponding to the carbohydrate signal together with that of phosphates and silicates. Silicates are minerals characterised by the presence of the tetrahedral group $(SiO_4)^{-4}$ and are abundant in the sediment where foraminifera live, and with which agglutinated foraminifera build their shells. Particularly, this variation (decrease of the peak in the spectrum) could represent, from lethal to sublethal concentration, a phase change of the minerals composing the *T. agglutinans* test associated with a change in both the calcitic cement and the organic component of the shell.

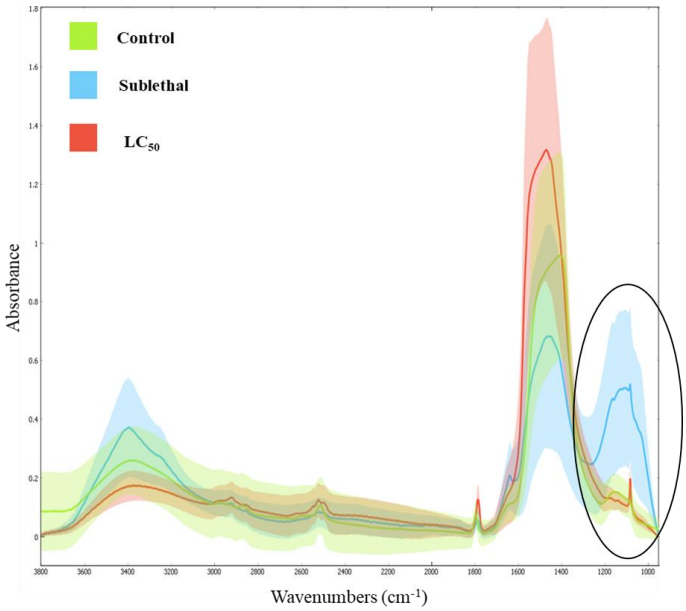

Figure 31. Average spectra of all *T. agglutinans* analysed samples. Circled peaks represent the signal from carbohydrates, phosphates and silicates (wavelength range 1000-1200 cm^1).

The above hypothesis does not take into account the macromolecular variations of the control specimen shells.

Considering the trend of the control samples, another foraminiferal response, related to the shell composition could be supposed. The carbohydrate and calcium carbonate contents show similar values both for exposure to the lethal concentration and under normal conditions (Figure 29). The situation changes markedly, however, when *T. agglutinans* is subjected to the sublethal concentration (Figure 29, carbohydrate content increases and calcium carbonate decreases sharply respectively). This would suggest that, at the synthetic nicotine lethal dose, biochemical conditions remain unchanged, i.e.,

the foraminifera die instantly without triggering survival strategies. In contrast, when exposure is sublethal, foraminifera respond by increasing the production of carbohydrates (i.e., mucopolysaccharides) of the entire organic matrix or IOL against an increase in the decalcification of the calcium carbonate cement and by keeping the mineral phase of the silicates stable.

Rosalina globularis, differently from *T. agglutinans*, responds by producing more calcium carbonate of its shell and carbohydrates when exposed to sublethal than lethal concentrations (Figure 32). Again, it could be assumed that the increase in the polysaccharide component of the shell organic matrix, during exposure to the sublethal concentration, is a cellular biochemical response to increase the IOL defences against the accumulation of synthetic nicotine in the cell. In this respect, the behaviour of *R. globularis* is like that of *T. agglutinans* (concerning the carbohydrates content) since the cell responds more actively when exposed to the sublethal concentration than to the lethal one, which is similar to the control (Figure 32). Further, the shell calcium carbonate decalcification seems to be more evident for individuals exposed to the lethal concentration than both the control and the sublethal concentration.

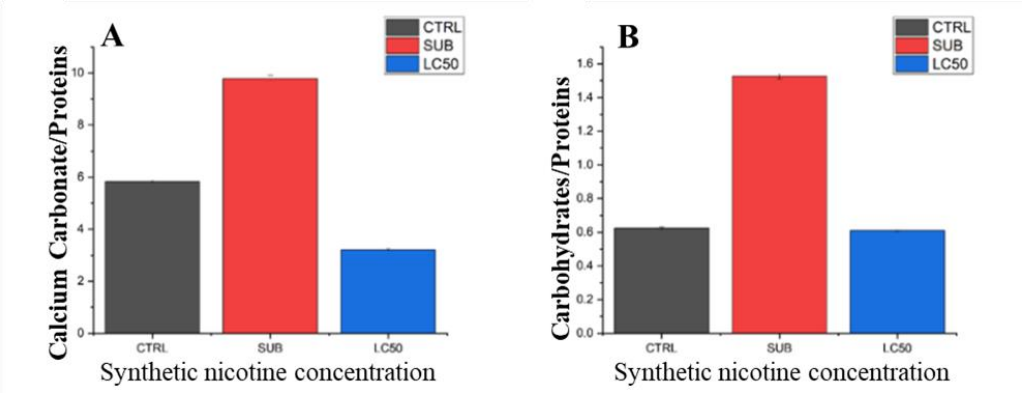

Figure 32. Histograms of the ratios Calcium carbonate/proteins and Carbohydrates/proteins for all samples of *R. globularis*.

However, FTIR data not only supported the hypothesis of foraminiferal shell decalcification, but also showed the presence of cellular stress on synthetic nicotine by modifying the organic component in the shell.

Considering the trend of the other macromolecules, lipids and proteins, whose variation indicates cellular stress, the two agglutinated and calcareous species show a similar response to synthetic nicotine. The total lipid content (expressed as CH_2-CH_3 mean integral) increased in the LC_{50} compared with the sublethal concentration and the control (Figure 33). From literature we know that an increase in lipid concentration is a signal for the initiation of the apoptotic process (Boren and Brindle, 2012). Apoptosis is indeed associated with an early accumulation of neutral lipids mostly in the form of cytoplasmic droplets (Al-Saffar et al., 2002) and the increase in CH_2-CH_3 signal intensity ratio of fatty acids correlates with the onset of apoptosis (Schmitz et al.,

2005). Further, cellular neutral lipids sustain the sequence of blebbing and formation of apoptotic bodies in cells dying by apoptosis and drive the synthesis of autophagosomal membranes in autophagy (Cristea and Degli Esposti, 2004; Crimi and Degli Esposti, 2011).

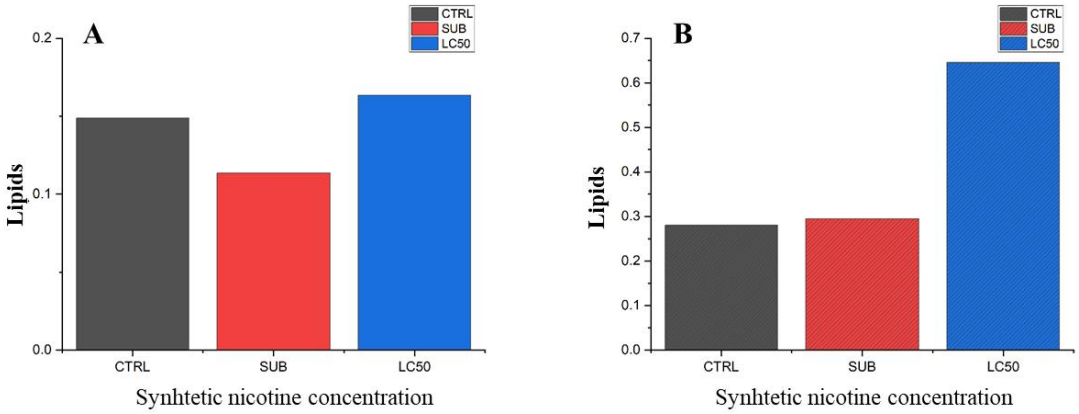

Figure 33. Total lipid content comparison charts for *T. agglutinans* (A) and *R. globularis* (B).

Regarding proteins, both foraminiferal species were subjected to a decrease in cytoplasmic proteins. In *T. agglutinans* it is more evident that the LC_{50} suffered a greater decrease in proteins than the sublethal (Figure 34A arrow), whereas *R. globularis* showed a more uneven pattern, in which the difference in protein content was less pronounced (the LC_{50} had slightly more protein than the sublethal) (Figure 34B arrow).

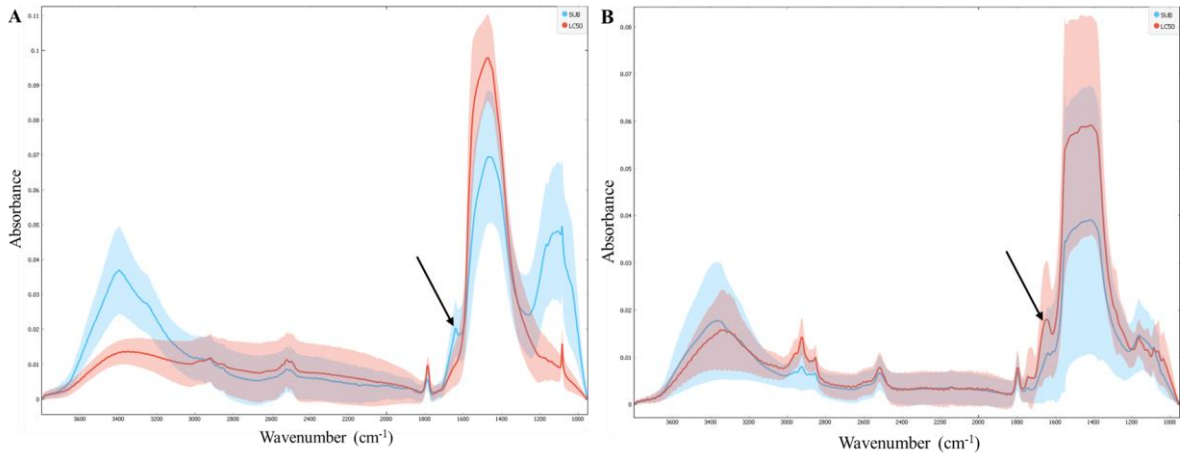

Figure 34. A) Sublethal and LC_{50} spectra of *T. agglutinans*.B) Sublethal and LC_{50} spectra of *R.globularis*.

Statistical analyses on *T. agglutinans* and *R. globularis* proteins (Figures 22 and 23 of Results) display that the toxicity of synthetic nicotine resulted not only in the protein content decrease but also in a drastic change in their structure. The range of protein wavelengths (1600-1700 cm^{-1}), in particular the peaks at wavenumber 1640 cm^{-1}, indicate the presence of amide I, which is the most studied band for the determination of proteins conformation (i.e., secondary structure) using FTIR (Barth et al., 2007; Ganim et al., 2008). Specifically, an increase in the high-wavenumber part of amide I is indicative of accumulating misfolded forms of proteins (Birarda et al., 2021), mostly β-sheet aggregates (Tidy et al., 2017), which are signals of cellular stress, leading also to apoptotic processes (Frontalini et al., 2015).

The histograms below (Figure 35) report FTIR data obtained by Caridi et al. (2020). Comparing them with FTIR data of this work, *R. globularis* results in

the same way sensitive to CB leachate and synthetic nicotine.

Individuals of *R. globularis*, with growing exposure to CB leachate, show decalcification, decreased cytoplasmic proteins and lipids, and reduced carbohydrates in the organic shell matrix (Figure 33).

Similarly, FTIR analyses of this thesis revealed the decalcification of *R. globularis* test, confirming the acidifying effect of synthetic nicotine and reaffirming the role of nicotine as the main intoxicating molecule in cigarette butts.

On the other hand, *T. agglutinans* was the least damaged species in the Caridi et al. work (2020), while it is particularly sensitive to synthetic nicotine pollution, as both lethal and sublethal doses of the latter caused shell weakening and the activation of cellular stress signals in this species.

This different behaviour influencing the macromolecules biochemistry, is probably related to the different solutions in which the foraminifera were incubated during the two experiments. In the LC_{50}-48 h test conducted by Caridi et al. (2020), the greater resistance of *T. agglutinans* compared to the two calcareous species (*R. globularis* and *Quinqueloculina* spp.) was determined by the increased production of calcium carbonate-cement and chitin to strengthen the test, and by the maintenance of its metabolic profile almost unchanged, indeed the lipid and protein content in the cytoplasm

exhibited a steady trend.

Contrarily, in the experiment of this master's degree thesis, *T. agglutinans* specimens underwent drastic changes in shell composition: sublethal specimens suffered a loss of calcium carbonate-cement, while LC_{50} specimens suffered a decrease in IOL polysaccharides. Furthermore, at the cellular level, synthetic nicotine dramatically altered metabolism, stimulating the accumulation of cytoplasmic lipids and misfolded proteins, both of which are signals of cellular stress and apoptotic process starting.

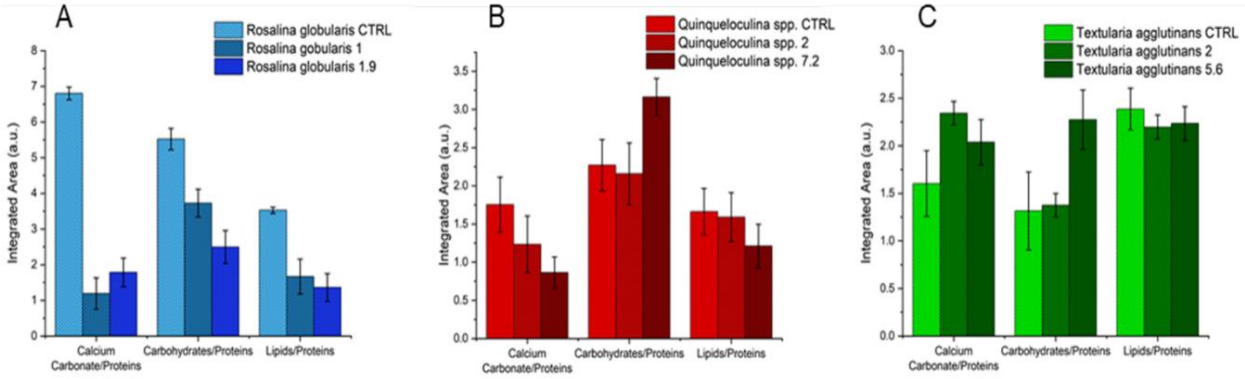

Figure 35. Histograms of the ratios Calcium carbonate/Proteins, Carbohydrates/Proteins and Lipids/Proteins for the three foraminiferal species considered. From left to right in order of sensitivity to the presence of cigarette leachates in the growth medium. A. In shades of blue, the bar chart represents the ratios of the band's integral average values for the *Rosalina globularis*. B. In shades of red, same representation for *Quinqueloculina* spp. data. C. In shades of green, bar chart representing the ratios of the band's integral average values for the *Textularia agglutinans*, the black bar represents standard error. For all the cigarette filters increase in concentration is represented by the darkening of the colour of the bar. Legend numbers are related to control, sublethal and lethal concentration of cigarette butts/L for the three species as specified in the section 2.4 and in the Tab. 2.

The impact of nicotine in the sea represents an extremely important issue for other marine organisms as well, which may react to the action of this emerging pollutant by decalcifying if they have calcium carbonate shells or exoskeletons (e.g., corals, molluscs, crustaceans), or by metabolising nicotine (converting it to cotinine) such as fish (Chang et al., 2015) and polychaetes (Wright et al., 2015).

Unfortunately, the mechanism of calcium carbonate dissolution in marine organisms by nicotine is not known.

In humans, cigarette consumption has been identified as a risk factor for bone mineral density (BMD) loss and osteoporotic fractures (Krall and Dawson-Hughes, 1999). Nicotine hinders osteogenesis, as it activates the expression of nicotinic receptors (Tanaka et al., 2013) and binds to calcium channels, preventing calcium accumulation and thus bone mineralisation.

According to Tanaka et al. (2005), nicotine is responsible for reducing the catalytic activity of alkaline phosphatase (an enzyme that hydrolyses substances that inhibit calcification and provides the phosphate required for hydroxyapatite crystallisation) and the production of type I collagen by osteoblasts. In addition, high concentrations of nicotine, acting directly on osteoclast precursors, inhibit the differentiation of human osteoclasts and promote bone resorption (Costa-Rodrigues, 2018).

Concerning foraminifera, analyses revealed that decalcification caused by nicotine does not correlate (or at least not completely) with the pH of the stock solution; indeed, in both LC_{50}-48 h tests, the pH decrease following incubation of foraminifera in the synthetic nicotine stock solution was minimal (the maximum decrease in pH was 0.10 in *R. globularis* sublethal R3, from 8.33 to 8.23).

Previous studies have proved that some enzymes involved in the biocalcification of pluricellular marine organisms are also present in foraminifera.

In an experiment on the perforated calcareous species *Amphistegina lessonii*, de Goeyse et al. (2021) found that in benthic foraminifera, intracellular carbonic anhydrase promotes calcification by increasing the rate of CO_2 converted to bicarbonate. Toyofuku et al. (2017) discovered that, at the site of shell calcification, excess protons from the conversion of CO_2 to (bi)carbonate are transported outside the foraminifera by the V-type H^+ ATPase enzyme.

From these observations, it was hypothesised that nicotine may have entered the membrane channels of foraminifera and interfered with the enzymes mentioned above.

Specifically, nicotine, upon reaching the calcification site, may have interrupted the outward proton flow generated by the V-type H^+ ATPase, resulting in protons increase within the test. These, together with protons produced by carbonic anhydrase (through the catalysis of CO_2 to bicarbonate), would have developed an acidic environment, which the foraminifera exploited to neutralise the effect of nicotine. As a result, the foraminifera weakened their shell. This stress may also have extended to the cell: the nicotine may have altered the foraminiferal metabolism to such an extent that the calcium carbonate of the test was required as a buffer.

Another hypothesis is that nicotine may have activated enzymes catalysing the synthesis of acid molecules, which in turn would have weakened the foraminifera shell by directly dissolving calcium carbonate.

In the light of the scenario just described, the results obtained in this master's degree thesis suggest that foraminifera are sensitive to decalcification due to the presence of pollutants such as nicotine and pH variation. The elaborated data refer to a cultured system, but it cannot be excluded that there is also an effect in a natural system where, alongside the progressive acidification of the water due to climate and anthropogenic change (Zeebe et al., 2016), the accumulation of pollutants such as nicotine can accelerate the dissolution process of calcium carbonate. The consequence is a reduction in the calcium

carbonate flow available to the marine ecosystem (Prazers et al., 2015; Byrne and Fitzer, 2019; Dobaradan et al., 2021).

Finally, the work fulfilled for this master's degree thesis helped to demonstrate that foraminifera can represent a good indicator for cigarette butts pollution in sea and that nicotine is an emerging pollutant causing cellular stress and shell damage in foraminifera.

Comparing the obtained results with the few ecotoxicological studies on other marine organisms belonging to different phyla, it is inferable that foraminifera are more resistant to the impact of substances contained in cigarette butts, primarily nicotine.

Performing liquid chromatography and tandem mass spectrometry (LC-MS/MS) analyses, Chang et al. (2015) determined the amount of nicotine and cotinine in fish (tuna and salmon) tissue extracts containing three different concentrations (37.5, 375 and 750 ng/g) of nicotine or cotinine. High recoveries of both molecules were achieved at all three concentrations, ranging from 70% to 120%. The same method was then applied for 24 hours to 15 *Pimephales promelas* specimens placed in aquaria containing 1 mg/L of nicotine. As a result, the concentration of accumulated nicotine increased with increasing nicotine exposure hours, reaching a maximum of approximately 4 μg/g, while cotinine maintained lower values of less than 1 μg/g.

Lethal concentrations (LC_{50}) of synthetic nicotine used in the December 2020 and April 2021 acute toxicity tests (LC_{50}-48 h) are 3.72 mg/L for *R. globularis*, 14.11 mg/L for *Quinqueloculina* spp. and 10.98 mg/L for *T. agglutinans*. These values correspond to 1.9, 7.2 and 5.6 butts/L respectively, and are higher than the LC_{50} doses found for other marine species using cigarette butts instead of synthetic nicotine.

Wright et al. (2015) incubated specimens of the species *Hediste diversicolor* (ragworm) for 96 hours in artificial seawater stock solutions at increasing concentrations of smoked cigarette filters. They reported that the nicotine concentration in the leachate containing the largest number of filters (8 filters/L) was 694 ng/mL. At this concentration, high nicotine:cotinine ratio was measured in the polychaetes, indicating that nicotine metabolism in ragworms was severely impaired due to the toxic substances contained in filters.

Slaughter et al. (2011) detected that the LC_{50} dose for leachate from smoked cigarette butts was 1.1 butts/L for the marine topsmelt *Atherinops affinis*.

Micevska et al. (2006) demonstrated that solutions consisting of cigarette butts of various brands were acutely toxic to the bacterium *Vibrio fischeri* at concentrations between 104 and 832 mg of butts/L, a range corresponding to 0.3-2.7 butts/L (30-minute EC_{50} (bioluminescence)).

6. CONCLUSIONS

This study represents the first attempt to assess the toxicity of synthetic nicotine on marine cultured microorganisms.

The results obtained in this master's degree thesis demonstrated that synthetic nicotine at both sublethal and lethal concentrations (LC_{50}) affects the viability, shell-building mechanism, and cell macromolecular composition of the three studied foraminiferal species: the perforated calcareous *Rosalina globularis*, the imperforate calcareous (miliolid) *Quinqueloculina* spp., and the agglutinated foraminifer *Textularia agglutinans*.

The two LC_{50}-48 h tests revealed that synthetic nicotine is acutely toxic to the three foraminiferal species, each of which exhibited a specific response linked to the type of shell biomineralization.

HPLC analyses confirmed that foraminifera absorbed much of the synthetic nicotine in the samples but were unable to convert it to cotinine within 48 hours. Furthermore, as shown by the FTIR analyses conducted on *T. agglutinans* and *R. globularis*, synthetic nicotine promotes shell decalcification and alters the composition of cytoplasmic macromolecules (i.e., lipids and proteins) of foraminifera subjected to this emerging pollutant.

However, the comparison of the results obtained with ecotoxicological studies performed with other marine organisms allowed us to establish that benthic foraminifera may represent an important bioindicator for pollution by cigarette butts in the sea.

All the data acquired to develop the present work derive from experimental observations carried out in the laboratory. The next step in deepening the effects of cigarette butt pollution on benthic foraminifera is to combine laboratory experiments with field studies.

REFERENCES

Al-Saffar, N. M. S., Titley, J. C., Robertson, D., Clarke, P. A., Jackson, L. E., Leach, M. O., & Ronen, S. M. (2002). Apoptosis is associated with triacylglycerol accumulation in Jurkat T-cells. *British journal of cancer*, *86*(6), 963-970.

Anderson O.R., Bé, A.W.H., 1978a. Recent advances in foraminiferal fine structure research. Foraminifera 3, 121-202.

Araújo, M. C. B., & Costa, M. F. (2019). A critical review of the issue of cigarette butt pollution in coastal environments. *Environmental research*, *172*, 137-149.

Banner, F. T., Sheehan, R., & Williams, E. (1973). The organic skeletons of rotaline foraminifera; a review. *The Journal of Foraminiferal Research*, *3*(1), 30-42.

Barth, A. (2007). Infrared spectroscopy of proteins. *Biochimica et Biophysica Acta (BBA)-Bioenergetics*, *1767*(9), 1073-1101.

Beaty, N. (2006). Lyophilization: heat and mass transfer. *American Pharmaceutical Review*, *9*, 81-83.

Bernhard, J. M., Ostermann, D. R., Williams, D. S., & Blanks, J. K. (2006). Comparison of two methods to identify live benthic foraminifera: A test between Rose Bengal and CellTracker Green with implications for stable isotope paleoreconstructions. *Paleoceanography*, *21*(4).

Birarda, G., Buosi, C., Caridi, F., Casu, M. A., De Giudici, G., Di Bella, L., ... & Vaccari, L. (2021). Plastics,(bio) polymers and their apparent biogeochemical cycle: An infrared spectroscopy study on foraminifera. *Environmental Pollution*, *279*, 116912.

Boltovskoy, E., 1964. Seasonal occurrences of some living foraminifera in Puerto Deseado (Patagonia, Argentina). *Journal du conseil international pour l'exporation de la mer, 29*: 136- 45.

Boren, J., & Brindle, K. M. (2012). Apoptosis-induced mitochondrial dysfunction causes cytoplasmic lipid droplet formation. *Cell Death & Differentiation*, *19*(9), 1561-1570.

Boyd, C. E. (2005). LC50 calculations help predict toxicity. *Global aquaculture advocate*, *8*(1), 84-87.

Byrne, M., & Fitzer, S. (2019). The impact of environmental acidification on the microstructure and mechanical integrity of marine invertebrate skeletons. *Conservation physiology*, *7*(1), coz062.

Caridi, F., Sabbatini, A., Birarda, G., Costanzi, E., De Giudici, G., Galeazzi, R., ... & Negri, A. (2020). Cigarette butts, a threat for marine environments: Lessons from benthic foraminifera (Protista). *Marine Environmental Research*, *162*, 105150.

Cau, A., Avio, C. G., Dessì, C., Moccia, D., Pusceddu, A., Regoli, F., ... & Follesa, M. C. (2020). Benthic crustacean digestion can modulate the environmental fate of microplastics in the deep sea. *Environmental science & technology*, *54*(8), 4886-4892.

Cecchini, M., & Changeux, J. P. (2015). The nicotinic acetylcholine receptor and its prokaryotic homologues: Structure, conformational transitions & allosteric modulation. *Neuropharmacology*, *96*, 137-149.

Chang, Y. W., Nguyen, H. P., Chang, M., Burket, S. R., Brooks, B. W., & Schug, K. A. (2015). Determination of nicotine and its metabolites accumulated in fish tissue using hydrophilic interaction liquid chromatography coupled with tandem mass spectrometry. *Journal of separation science*, *38*(14), 2414-2422.

Ciacci, C., Grimmelpont, M. V., Corsi, I., Bergami, E., Curzi, D., Burini, D., ... & Frontalini, F. (2019). Nanoparticle-biological interactions in a marine benthic foraminifer. *Scientific reports*, *9*(1), 1-10.

Costa-Rodrigues, J., Rocha, I., & Fernandes, M. H. (2018). Complex osteoclastogenic inductive effects of nicotine over hydroxyapatite. *Journal of cellular physiology*, *233*(2), 1029-1040.

Crimi, M., & Degli Esposti, M. (2011). Apoptosis-induced changes in mitochondrial lipids. *Biochimica et Biophysica Acta (BBA)-Molecular Cell Research*, *1813*(4), 551-557.

Cristea, I. M., & Degli Esposti, M. (2004). Membrane lipids and cell death: an overview. *Chemistry and Physics of Lipids*, *129*(2), 133-160.

Curtis, C., Novotny, T. E., Lee, K., Freiberg, M., & McLaughlin, I. (2017). Tobacco industry responsibility for butts: a model tobacco waste act. *Tobacco control*, *26*(1), 113-117.

de Freitas Prazeres, M., Martins, S. E., & Bianchini, A. (2011). Biomarkers response to zinc exposure in the symbiont-bearing foraminifer Amphistegina lessonii (Amphisteginidae, Foraminifera). *Journal of Experimental Marine Biology and Ecology*, *407*(1), 116-121.

de Goeyse, S., Webb, A. E., Reichart, G. J., & de Nooijer, L. J. (2021). Carbonic anhydrase is involved in calcification by the benthic foraminifer Amphistegina lessonii. *Biogeosciences*, *18*(2), 393-401.

de Nooijer, L. J., Spero, H. J., Erez, J., Bijma, J., & Reichart, G. J. (2014). Biomineralization in perforate foraminifera. *Earth-Science Reviews*, *135*, 48-58.

de Nooijer, L. J., Toyofuku, T., Oguri, K., Nomaki, H., & Kitazato, H. (2008). Intracellular pH distribution in foraminifera determined by the fluorescent probe HPTS. *Limnology and Oceanography: Methods*, *6*(11), 610-618.

de Nooijer, L. J., Toyofuku, T., & Kitazato, H. (2009). Foraminifera promote calcification by elevating their intracellular pH. *Proceedings of the National Academy of Sciences*, *106*(36), 15374-15378.

Dieng, H., Rajasaygar, S., Ahmad, A. H., Ahmad, H., Rawi, C. S. M., Zuharah, W. F., ... & AbuBakar, S. (2013). Turning cigarette butt waste into an alternative control tool against an insecticide-resistant mosquito vector. *Acta tropica*, *128*(3), 584-590.

Dieng, H., Rajasaygar, S., Ahmad, A. H., Rawi, C. S. M., Ahmad, H., Satho, T., ... & AbuBakar, S. (2014). Indirect effects of cigarette butt waste on the dengue vector Aedes aegypti (Diptera: Culicidae). *Acta tropica*, *130*, 123-130.

Dobaradaran, S., Soleimani, F., Akhbarizadeh, R., Schmidt, T. C., Marzban, M., & BasirianJahromi, R. (2021). Environmental fate of cigarette butts and

their toxicity in aquatic organisms: A comprehensive systematic review. *Environmental Research*, 110881.

Erez, J. (2003). The source of ions for biomineralization in foraminifera and their implications for paleoceanographic proxies. *Reviews in mineralogy and geochemistry*, *54*(1), 115-149.

Frontalini, F., & Coccioni, R. (2012). The response of benthic foraminiferal assemblages to copper exposure: a pilot mesocosm investigation. *Journal of Environmental Protection*, *2012*.

Frontalini, F., Curzi, D., Giordano, F. M., Bernhard, J. M., Falcieri, E., & Coccioni, R. (2015). Effects of lead pollution on Ammonia parkinsoniana (foraminifera): ultrastructural and microanalytical approaches. *European journal of histochemistry: EJH*, *59*(1).

Frontalini, F., Greco, M., Di Bella, L., Lejzerowicz, F., Reo, E., Caruso, A., ... & Pawlowski, J. (2018). Assessing the effect of mercury pollution on cultured benthic foraminifera community using morphological and eDNA metabarcoding approaches. *Marine pollution bulletin*, *129*(2), 512-524.

Frontalini, F., Semprucci, F., Di Bella, L., Caruso, A., Cosentino, C., Maccotta, A., ... & Coccioni, R. (2018). The response of cultured meiofaunal and benthic foraminiferal communities to lead exposure: Results from mesocosm experiments. *Environmental toxicology and chemistry*, *37*(9), 2439-2447.

Ganim, Z., Chung, H. S., Smith, A. W., DeFlores, L. P., Jones, K. C., & Tokmakoff, A. (2008). Amide I two-dimensional infrared spectroscopy of proteins. *Accounts of chemical research*, *41*(3), 432-441.

Gomes, I. B., Simões, L. C., & Simões, M. (2018). The effects of emerging environmental contaminants on Stenotrophomonas maltophilia isolated from drinking water in planktonic and sessile states. *Science of the total environment*, *643*, 1348-1356.

Harvey, B. P., Agostini, S., Wada, S., Inaba, K., & Hall-Spencer, J. M. (2018). Dissolution: the Achilles' heel of the triton shell in an acidifying ocean. *Frontiers in Marine Science*, *5*, 371.

Hottinger, L. (2006). Illustrated glossary of terms used in foraminiferal research. Carnets de Géologie/Notebooks on Geology-Memoir 2006/02.

Issakhov, A., & Zhandaulet, Y. (2019). Numerical simulation of thermal pollution zones' formations in the water environment from the activities of the power plant. *Engineering Applications of Computational Fluid Mechanics*, *13*(1), 279-299.

Jorissen, F., Nardelli, M. P., Almogi-Labin, A., Barras, C., Bergamin, L., Bicchi, E., ... & Spezzaferri, S. (2018). Developing Foram-AMBI for biomonitoring in the Mediterranean: species assignments to ecological categories. *Marine Micropaleontology*, *140*, 33-45.

Keul, N., & Schmidt, S. (2018, December). Calcification in foraminifera largely supported by ion channels-biomineralization pathways and their effect on trace elemental composition. In *AGU Fall Meeting Abstracts* (Vol. 2018, pp. PP43A-02).

Krall, E. A., & Dawson-Hughes, B. (1999). Smoking increases bone loss and decreases intestinal calcium absorption. *Journal of Bone and Mineral Research*, *14*(2), 215-220.

Langlet, D., Bouchet, V. M., Delaeter, C., & Seuront, L. (2020). Motion behavior and metabolic response to microplastic leachates in the benthic foraminifera Haynesina germanica. *Journal of Experimental Marine Biology and Ecology*, *529*, 151395.

Lee, J., 2012. Get Your Butt off the Ground!: Consequences of Cigarette Waste and Litter-Reducing Methods.

Lee, W., & Lee, C. C. (2015). Developmental toxicity of cigarette butts–An underdeveloped issue. *Ecotoxicology and environmental safety*, *113*, 362-368.

Li, J., Liu, H., & Chen, J. P. (2018). Microplastics in freshwater systems: A review on occurrence, environmental effects, and methods for microplastics detection. *Water research*, *137*, 362-374.

Loeblich, A.R. Tappan, H., 1964. Sarcodina, chiefly "Thecamoebians" and Foraminiferida. In: Moore, R.C. (Ed.), Treatise on Invertebrate Paleontology. Part C. Geol. Soc. Amer. and Univ. Kansas, p. 900.

Loeblich, A.R. Tappan, H., 1988. Foraminiferal genera and their classification, vol. 1. Van Nostrand Reinhold Company, p. 970 vol. 2, pp. 212 + 847 pls.

Lombardi, C. C., Di Cicco, G., & Zagà, V. (2009). Le cicche di sigaretta: un rifiuto tossico dimenticato. *Tabaccologia*, *4*, 27-36.

Luo, Y., Guo, W., Ngo, H. H., Nghiem, L. D., Hai, F. I., Zhang, J., ... & Wang, X. C. (2014). A review on the occurrence of micropollutants in the aquatic environment and their fate and removal during wastewater treatment. *Science of the total environment*, *473*, 619-641.

Martinez Gomez, D. A., Baca, S., & Walsh, E. J. (2015). Lethal and sublethal effects of selected PPCPs on the freshwater rotifer, Plationus patulus. *Environmental toxicology and chemistry*, *34*(4), 913-922.

Matta, S. G., Balfour, D. J., Benowitz, N. L., Boyd, R. T., Buccafusco, J. J., Caggiula, A. R., ... & Zirger, J. M. (2007). Guidelines on nicotine dose selection for in vivo research. *Psychopharmacology*, *190*(3), 269-319.

Micevska, T., Warne, M. S. J., Pablo, F., & Patra, R. (2006). Variation in, and causes of, toxicity of cigarette butts to a cladoceran and microtox. *Archives of Environmental Contamination and Toxicology*, *50*(2), 205-212.

Moerman, J. W., & Potts, G. E. (2011). Analysis of metals leached from smoked cigarette litter. *Tobacco control*, *20*(Suppl 1), i30-i35.

Murray, J. W., 1991. Ecology and Palaeoecology of Benthic Foraminifera. Harlow: Longman. Scientific & Technical, 397 pp.

Nardelli, M. P., Sabbatini, A., & Negri, A. (2013). Experimental chronic exposure of the foraminifer Pseudotriloculina rotunda to zinc. *Acta Protozoologica*, *52*(3).

Novotny, T. E., Lum, K., Smith, E., Wang, V., & Barnes, R. (2009). Cigarettes butts and the case for an environmental policy on hazardous cigarette waste. *International journal of environmental research and public health*, *6*(5), 1691-1705.

Novotny, T. E., & Slaughter, E. (2014). Tobacco product waste: an environmental approach to reduce tobacco consumption. *Current environmental health reports*, *1*(3), 208-216.

Pati, P., & Patra, P. K. (2012). Benthic foraminiferal responses to coastal pollution: a review. *International Journal of Geology, Earth and Environmental Sciences*, *2*(1), 2277-2081.

Planet, L.F., 2009. Exposing the butts. Retrieved from Littoral society 25, 23-29.

Prazeres, M., Uthicke, S., & Pandolfi, J. M. (2015). Ocean acidification induces biochemical and morphological changes in the calcification process of large benthic foraminifera. *Proceedings of the royal society B: Biological sciences*, *282*(1803), 20142782.

Pucci, F., Geslin, E., Barras, C., Morigi, C., Sabbatini, A., Negri, A., & Jorissen, F. J. (2009). Survival of benthic foraminifera under hypoxic conditions: Results of an experimental study using the CellTracker Green method. *Marine Pollution Bulletin*, *59*(8-12), 336-351.

Quéméneur, M., Chifflet, S., Akrout, F., Bellaaj-Zouari, A., & Belhassen, M. (2020). Impact of cigarette butts on microbial diversity and dissolved trace metals in coastal marine sediment. *Estuarine, Coastal and Shelf Science*, *240*, 106785.

Ros, M. T. L., Al-Enezi, E., Cesarini, E., Canonico, B., Bucci, C., Martins, M. V. A., ... & Frontalini, F. (2020). Assessing the Cadmium Effects on the Benthic Foraminifer Ammonia cf. parkinsoniana: An Acute Toxicity Test. *Water*, *12*(4), 1018.

Ross, B. (2012). *Responses to chemical exposure by foraminifera: distinguishing dormancy from mortality*. University of South Florida.

Ross, B. J., & Hallock, P. (2016). Dormancy in the foraminifera: A review. *The Journal of Foraminiferal Research*, *46*(4), 358-368.

Ross, B. J., & Hallock, P. (2018). Challenges in using CellTracker Green on foraminifers that host algal endosymbionts. *PeerJ*, *6*, e5304.

Sabbatini, A., Bédouet, L., Marie, A., Bartolini, A., Landemarre, L., Weber, M. X., ... & Vénec-Peyré, M. T. (2014). Biomineralization of S chlumbergerella floresiana, a significant carbonate-producing benthic foraminifer. *Geobiology*, *12*(4), 289-307.

Santos, I. R., Friedrich, A. C., Wallner-Kersanach, M., & Fillmann, G. (2005). Influence of socio-economic characteristics of beach users on litter generation. *Ocean & Coastal Management*, *48*(9-10), 742-752.

Schmitz, J. E., Kettunen, M. I., Hu, D. E., & Brindle, K. M. (2005). 1H MRS-visible lipids accumulate during apoptosis of lymphoma cells in vitro and in vivo. *Magnetic Resonance in Medicine: An Official Journal of the International Society for Magnetic Resonance in Medicine*, *54*(1), 43-50.

Sen Gupta, B. K. (1999). Systematics of moder Foraminifera. In *Modern foraminifera* (pp. 7-36). Springer, Dordrecht.

Shen, M., Li, Y., Song, B., Zhou, C., Gong, J., & Zeng, G. (2021). Smoked cigarette butts: Unignorable source for environmental microplastic fibers. *Science of The Total Environment*, *791*, 148384.

Slaughter, E., Gersberg, R. M., Watanabe, K., Rudolph, J., Stransky, C., & Novotny, T. E. (2011). Toxicity of cigarette butts, and their chemical components, to marine and freshwater fish. *Tobacco control*, *20*(Suppl 1), i25-i29.

Sobrino-Figueroa, A. (2015). Toxic effects of emerging pollutants in juveniles of the freshwater gastropod Physa acuta (Draparnaud, 1805). *American Malacological Bulletin*, *33*(2), 337-342.

Tanaka, H., Tanabe, N., Suzuki, N., Shoji, M., Torigoe, H., Sugaya, A., ... & Maeno, M. (2005). Nicotine affects mineralized nodule formation by the human osteosarcoma cell line Saos-2. *Life sciences*, *77*(18), 2273-2284.

Tanaka, H., Tanabe, N., Kawato, T., Nakai, K., Kariya, T., Matsumoto, S., ... & Maeno, M. (2013). Nicotine affects bone resorption and suppresses the expression of cathepsin K, MMP-9 and vacuolar-type H+-ATPase d2 and actin organization in osteoclasts. *PloS one*, *8*(3), e59402.

Tang, Y., Yin, M., Yang, W., Li, H., Zhong, Y., Mo, L., ... & Sun, X. (2019). Emerging pollutants in water environment: Occurrence, monitoring, fate, and risk assessment. *Water Environment Research*, *91*(10), 984-991.

Tidy, R. J., Lam, V., Fimognari, N., Mamo, J. C., & Hackett, M. J. (2017). FTIR studies of the similarities between pathology induced protein aggregation in vivo and chemically induced protein aggregation ex vivo. *Vibrational Spectroscopy*, *91*, 68-76.

Torkashvand, J., Farzadkia, M., Sobhi, H. R., & Esrafili, A. (2020). Littered cigarette butt as a well-known hazardous waste: a comprehensive systematic review. *Journal of hazardous materials*, *383*, 121242.

Toyofuku, T., Matsuo, M. Y., De Nooijer, L. J., Nagai, Y., Kawada, S., Fujita, K., ... & Kitazato, H. (2017). Proton pumping accompanies calcification in foraminifera. *Nature Communications*, *8*(1), 1-6.

Traverse, A. (2007). *Paleopalynology* (Vol. 28). Springer Science & Business Media.

Tyszka, J., Godos, K., Goleń, J., & Radmacher, W. (2021). Foraminiferal organic linings: Functional and phylogenetic challenges. *Earth-Science Reviews*, *220*, 103726.

Vasilachi, I. C., Asiminicesei, D. M., Fertu, D. I., & Gavrilescu, M. (2021). Occurrence and fate of emerging pollutants in water environment and options for their removal. *Water*, *13*(2), 181.

Vickerman, K., 1992. The diversity and ecological significance of Protozoa. *Biodiversity and Conservation, 1*: 334-341.

Walton, W. R., 1964. Ecology of benthonic foraminifera in the Tampa-Sarasota Bay area, Florida. In: Miller, R. L., (Ed.) Papers in Marine Geology. New York: Macmillan, 429-54.

Wright, S. L., Rowe, D., Reid, M. J., Thomas, K. V., & Galloway, T. S. (2015). Bioaccumulation and biological effects of cigarette litter in marine worms. *Scientific reports*, *5*(1), 1-10.

Zamora-Duran, M. A., Aronson, R. B., Leichter, J. J., Flannery, J. A., Richey, J. N., & Toth, L. T. (2020). Imprint of Regional Oceanography on

Foraminifera of Eastern Pacific Coral Reefs. *Journal of Foraminiferal Research*, *50*(3), 279-290.

Zeebe, R. E., Ridgwell, A., & Zachos, J. C. (2016). Anthropogenic carbon release rate unprecedented during the past 66 million years. *Nature Geoscience*, *9*(4), 325-329.

FTIR SUPPLEMENTARY DATA

Samples employed in Fourier Transform Infrared (FTIR) analyses

SAMPLE NAME	DESCRIPTION
Textularia sub R3 US	*Textularia agglutinans* - sublethal replicate 3 - unstained
Textularia sub R3 US	*Textularia agglutinans* - sublethal replicate 3 - unstained
Textularia LC_{50} R3 US	*Textularia agglutinans* - LC_{50} replicate 3 - unstained
Textularia LC_{50} R3 US	*Textularia agglutinans* - LC_{50} replicate 3 - unstained
Quinqueloculina CTRL US	*Quinqueloculina* spp. - control - unstained
Quinqueloculina LC_{50} R3 US	*Quinqueloculina* spp. - LC_{50} replicate 3 - unstained
Quinqueloculina LC_{50} R3 US	*Quinqueloculina* spp. - LC_{50} replicate 3 - unstained
Rosalina CTRL US	*Rosalina globularis* - control - unstained
Rosalina sub R3 US	*Rosalina globularis* - sublethal replicate 3 - unstained
Rosalina sub R3 US	*Rosalina globularis* - sublethal replicate 3 - unstained
Rosalina LC_{50} R3 US	*Rosalina globularis* - LC_{50} replicate 3 - unstained
Rosalina LC_{50} R3 US	*Rosalina globularis* - LC_{50} replicate 3 - unstained
Textularia LC_{50} solution	*Textularia agglutinans* - LC_{50} - solution
Quinqueloculina sub solution	*Quinqueloculina* spp. - sublethal - solution
Quinqueloculina LC_{50} solution	*Quinqueloculina* spp. - LC_{50} - solution
Rosalina sub solution	*Rosalina globularis* - sublethal - solution
Rosalina LC_{50} solution	*Rosalina globularis* - LC_{50} - solution
Textularia CRTL CTG	*Textularia agglutinans* - control - Cell Tracker Green
Textularia LC_{50} R1 CTG	*Textularia agglutinans* - LC_{50} replicate 1 - Cell Tracker Green
Quinqueloculina LC_{50} R1 CTG	*Quinqueloculina* spp. - LC_{50} replicate 1 - Cell Tracker Green